Supplementary Information on

Bismuth as Versatile Cation for Luminescence in Coordination Polymers from BiX_3/4,4'-bipy: Understanding of Photophysics by Quantum Chemical Calculations and Structural Parallels to Lanthanides

Jens R. Sorg,[a] Tobias Wehner,[a] Philipp R. Matthes,[a] Rebecca Sure[b], Stefan Grimme,[b] Johanna Heine,[c] and Klaus Müller-Buschbaum[a]

a Institute of Inorganic Chemistry, Julius-Maximilians-University Würzburg, Am Hubland, 97074 Würzburg, Germany.

b Mulliken Center for Theoretical Chemistry, Institut für Physikalische und Theoretische Chemie der Rheinischen Friedrich-Wilhelms, Universität Bonn, Beringstr. 4, 53115 Bonn, Germany

c Department of Chemistry and Material Sciences Center, Philipps-Universität Marburg, Hans-Meerwein-Straße, 35043 Marburg, Germany.

Crystallography

Crystallographic details for 1a

Table S1: Crystallographic data for **1a**.

	1a
Empirical formula	$C_{10}H_8BiCl_3N_2$
Formula weight /g·mol^{-1}	471.51
Crystal colour and shape	colourless block
Crystal size	0.2 × 0.15 × 0.1
Crystal system	monoclinic
Space group	*C*2/*c*
a /Å	10.0218(9)
b /Å	24.140(2)
c /Å	11.8811(10)
α /°	90
β /°	113.7320(10)
γ /°	90
V /Å^3	2631.3(4)
Z	8
ρ_{calc} /g·cm^{-3}	2.380
μ(Mo$_{K\alpha}$) /mm^{-1}	13.983
measurement temp. /K	100
Absorption correction type	multi-scan
Min/max transmission	0.4146/0.7460
2Θ range /°	3.374-60.234
No. of measured reflections	30068
No. of independent reflections	3869
R(int)	0.1574
No. of indep. reflections ($I > 2\sigma(I)$)	3497
No. of parameters	146
R_1 ($I > 2\sigma(I)$)	0.0395
wR_2 (all data)	0.1020
S (all data)	1.060
$\Delta\rho_{max}$, $\Delta\rho_{min}$ /e· Å^{-3}	5.85/-3.68

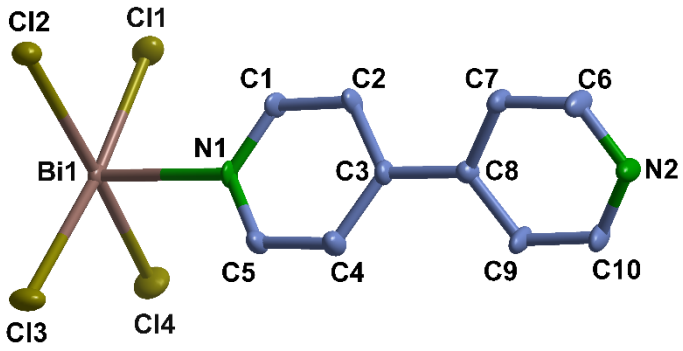

Figure S1: Asymmetric unit of **1a**, ellipsoids at 50% probability.

Table S2: Selected interatomic distances (in Å) and angles (in °) in **1a**.

Symmetry operations: I 1+x,+y,-1+z

Bi1 Cl3	2.9050(13)	Cl1 Bi1 Cl3	170.75(4)	N1 Bi1 Cl4	94.02(11)
Bi1 Cl2	2.8885(12)	Cl1 Bi1 Cl2	84.63(4)	$N2^{I}$ Bi1 Cl3	88.98(12)
Bi1 Cl1	2.5184(13)	Cl1 Bi1 Cl4	95.45(5)	$N2^{I}$ Bi1 Cl2	86.85(11)
Bi1 Cl4	2.5429(13)	Cl1 Bi1 N1	89.95(10)	$N2^{I}$ Bi1 Cl1	90.82(11)
Bi1 N1	2.539(4)	Cl4 Bi1 Cl3	93.80(5)	$N2^{I}$ Bi1 Cl4	90.25(11)
Bi1 $N2^{I}$	2.514(5)	Cl4 Bi1 Cl2	177.10(3)	$N2^{I}$ Bi1 N1	175.57(14)
		N1 Bi1 Cl3	89.56(10)		
Cl2 Bi1 Cl3	86.12(4)	N1 Bi1 Cl2	88.88(10)		

Crystallographic details for 1b

Table S3: Crystallographic data for **1b**.

	1b
Empirical formula	$C_{10}H_8BiCl_3N_2$
Formula weight /g·mol^{-1}	471.51
Crystal colour and shape	colourless block
Crystal size	0.218 × 0.144 × 0.133
Crystal system	triclinic
Space group	$P\bar{1}$
a /Å	8.1976(16)
b /Å	8.6395(17)
c /Å	9.7726(19)
α /°	66.75(3)
β /°	88.28(3)
γ /°	87.94(3)
V /Å^3	635.4(3)
Z	2
ρ_{calc} /g·cm^{-3}	2.465
μ(Mo$_{K\alpha}$) /mm^{-1}	14.477
measurement temp. /K	100
Absorption correction type	multi-scan
Min/max transmission	0.4906/0.7457
2Θ range /°	4.538-56.686
No. of measured reflections	9078
No. of independent reflections	3159
R(int)	0.0497
No. of indep. reflections ($I > 2\sigma(I)$)	2797
No. of parameters	145
R_1 ($I > 2\sigma(I)$)	0.0319
wR_2 (all data)	0.0684
S (all data)	1.003
$\Delta\rho_{max}$, $\Delta\rho_{min}$ /e· Å^{-3}	2.24/-1.86

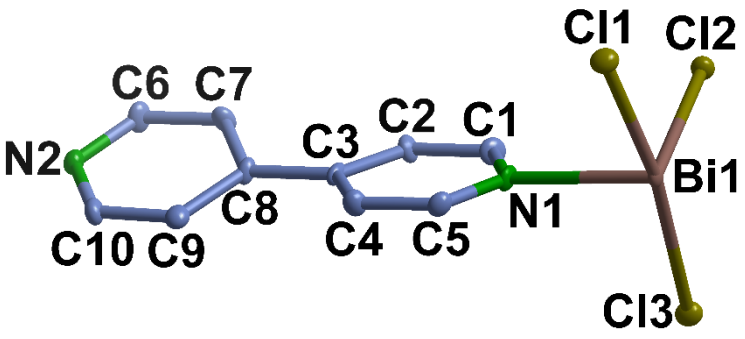

Figure S2: Asymmetric unit of **1b**, ellipsoids at 50% probability.

Table S4: Selected interatomic distances (in Å) and angles (in °) in **1b**.

Symmetry operations: I 2-x,1-y,1-z; II 1+x,1+y, z

Bi1 Cl2	2.5032(15)	Cl2 Bi1 $Cl3^{I}$	175.24(4)	N1 Bi1 Cl1	88.66(12)
Bi1 Cl1	2.5260(18)	Cl2 Bi1 Cl3	87.41(5)	N1 Bi1 $Cl3^{I}$	89.02(12)
Bi1 Cl3	2.921(2)	Cl2 Bi1 $N2^{II}$	88.93(12)	N1 Bi1 Cl3	83.50(12)
Bi1 $Cl3^{I}$	2.9413(16)	Cl1 Bi1 Cl3	171.98(4)	N1 Bi1 $N2^{II}$	177.87(15)
Bi1 N1	2.467(5)	Cl1 Bi1 $Cl3^{I}$	90.36(5)	N2 Bi1 $Cl3^{I}$	94.65(12)
Bi1 $N2^{II}$	2.575(5)	Cl1 Bi1 $N2^{II}$	93.22(12)	$N2^{II}$ Bi1 $Cl3^{I}$	91.96(12)
		Cl3 Bi1 $Cl3^{I}$	87.85(5)		
Cl2 Bi1 Cl1	94.26(5)	N1 Bi1 Cl2	89.94(12)		

Crystallographic details for 2

Table S5: Crystallographic data for **2**.

	2
Empirical formula	$C_{10}H_8BiBr_3N_2$
Formula weight /g·mol^{-1}	604.89
Crystal colour and shape	colourless block
Crystal size	0.205 × 0.091 × 0.067
Crystal system	triclinic
Space group	$P\bar{1}$
a /Å	8.0006(16)
b /Å	9.1231(18)
c /Å	10.094(2)
α /°	114.97(3)
β /°	92.83(3)
γ /°	90.59(3)
V /Å^3	666.7(3)
Z	2
ρ_{calc} /g·cm^{-3}	3.013
μ(Mo$_{K\alpha}$) /mm^{-1}	22.186
measurement temp. /K	100
Absorption correction type	multi-scan
Min/max transmission	0.4472/0.7457
2Θ range /°	4.458-56.97
No. of measured reflections	10278
No. of independent reflections	3379
R(int)	0.0235
No. of indep. reflections ($I > 2\sigma(I)$)	3162
No. of parameters	145
R_1 ($I > 2\sigma(I)$)	0.0189
wR_2 (all data)	0.0415
S (all data)	1.066
$\Delta\rho_{max}$, $\Delta\rho_{min}$ /e· Å^{-3}	1.26/-0.96

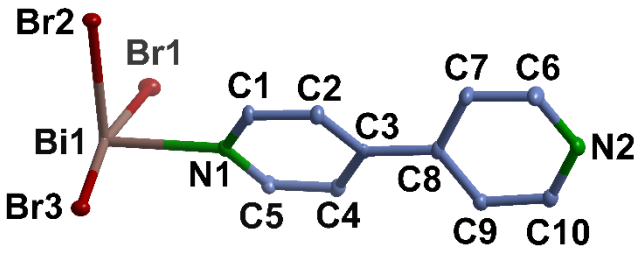

Figure S3: Asymmetric unit of **2**, ellipsoids at 50% probability.

Table S6: Selected interatomic distances (in Å) and angles (in °) in **2**.

Symmetry operations: I -x,1-y,1-z II -1+x,-1+y,z

Bi1 Br3	3.0325(14)	Br3 Bi1 Br3^{I}	88.54(3)	N2^{II} Bi1 Br2	89.97(7)
Bi1 Br3^{I}	3.0779(9)	Br2 Bi1 Br3	88.23(3)	N2^{II} Bi1 Br1	96.35(7)
Bi1 Br2	2.6437(8)	Br2 Bi1 Br3^{I}	176.767(11)	N1 Bi1 Br3^{I}	88.99(7)
Bi1 Br1	2.6667(12)	Br2 Bi1 Br1	93.82(3)	N1 Bi1 Br3	82.02(7)
Bi1 N2^{II}	2.592(3)	Br1 Bi1 Br3^{I}	89.36(3)	N1 Bi1 Br2	90.52(7)
Bi1 N1	2.454(3)	Br1 Bi1 Br3	169.588(13)	N1 Bi1 Br1	87.75(7)
Br3 Bi1^{I}	3.0780(9)	N2^{II} Bi1 Br3	93.86(7)	N1 Bi1 N2^{II}	175.83(9)
		N2^{II} Bi1 Br3	90.29(7)		

Crystallographic details for 3

Table S7: Crystallographic data for **3**.

	3
Empirical formula	$C_{10}H_8BiI_3N_2$
Formula weight /g·mol^{-1}	745.86
Crystal colour and shape	yellow block
Crystal size	0.28 × 0.161 × 0.153
Crystal system	triclinic
Space group	$P\bar{1}$
a /Å	7.6526(15)
b /Å	10.094(2)
c /Å	10.841(2)
α /°	117.34(3)
β /°	91.13(3)
γ /°	94.78(3)
V /Å^3	739.7(3)
Z	2
ρ_{calc} /g·cm^{-3}	3.349
μ(Mo$_{K\alpha}$) /mm^{-1}	18.157
measurement temp. /K	100
Absorption correction type	multi-scan
Min/max transmission	0.3589/0.7457
2Θ range /°	5.354-56.646
No. of measured reflections	10057
No. of independent reflections	3675
R(int)	0.0309
No. of indep. reflections ($I > 2\sigma(I)$)	3385
No. of parameters	145
R_1 ($I > 2\sigma(I)$)	0.0240
wR_2 (all data)	0.0499
S (all data)	1.051
$\Delta\rho_{max}$, $\Delta\rho_{min}$ /e· Å^{-3}	1.10/-1.37

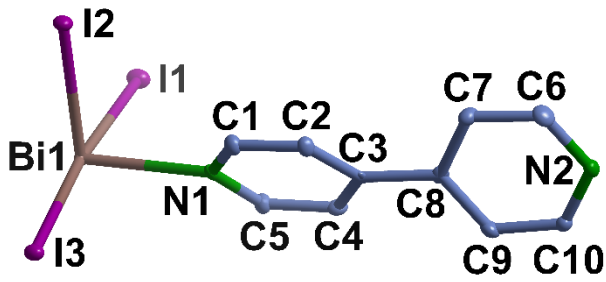

Figure S4: Asymmetric unit of **3**, ellipsoids at 50% probability.

Table S8: Selected interatomic distances (in Å) and angles (in °) in **3**.

Symmetry operations: I 1-x,1-y,1-z II -1+x,-1+y,+z

Bi1 $I3^{I}$	3.3339(10)	I2 Bi1 I3	89.12(3)	N1 Bi1 I2	89.98(10)
Bi1 I3	3.2137(14)	I2 Bi1 $I3^{I}$	177.846(11)	N1 Bi1 I1	90.34(10)
Bi1 I2	2.8706(9)	I2 Bi1 I1	92.85(3)	N1 Bi1 $N2^{II}$	173.19(13)
Bi1 I1	2.9178(13)	I1 Bi1 I3	174.215(11)	$N2^{II}$ Bi1 $I3^{I}$	90.60(9)
Bi1 N1	2.525(4)	I1 Bi1 $I3^{I}$	88.69(3)	$N2^{II}$ Bi1 I3	89.03(10)
Bi1 $N2^{II}$	2.585(4)	N1 Bi1 I3	84.21(10)	$N2^{II}$ Bi1 I2	90.73(9)
		N1 Bi1 $I3^{I}$	88.50(10)	$N2^{II}$ Bi1 I1	96.38(10)
I3 Bi1 $I3^{I}$	89.21(3)				

Crystallographic details for 4

Table S9: Crystallographic data for **4**.

	4
Empirical formula	$C_{20}H_{19}BiCl_4N_4$
Formula weight /g·mol^{-1}	666.17
Crystal colour and shape	colourless block
Crystal size	0.301 × 0.214 × 0.205
Crystal system	monoclinic
Space group	*C*2/*m*
a /Å	13.062(3)
b /Å	12.287(2)
c /Å	8.1125(15)
α /°	90
β /°	121.421(5)
γ /°	90
V /Å^3	1111.1(4)
Z	2
ρ_{calc} /g·cm^{-3}	1.991
μ(Mo$_{K\alpha}$) /mm^{-1}	8.430
measurement temp. /K	100
Absorption correction type	multi-scan
Min/max transmission	0.5223/0.7457
2Θ range /°	4.934-56.692
No. of measured reflections	8185
No. of independent reflections	1446
R(int)	0.0394
No. of indep. reflections ($I > 2\sigma(I)$)	1439
No. of parameters	73
R_1 ($I > 2\sigma(I)$)	0.0223
wR_2 (all data)	0.0554
S (all data)	1.173
$\Delta\rho_{max}$, $\Delta\rho_{min}$ /e· Å^{-3}	1.79/-1.71

Details of crystal structure refinement: The hydrogen atom attached to N2 has half occupancy to correctly model the pyridine·pyridinium homodimer.

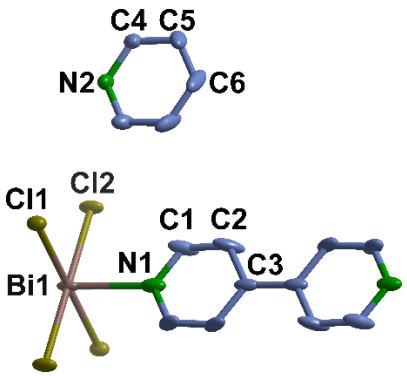

Figure S5: Asymmetric unit of **4**, ellipsoids at 50% probability.

Table S10: Selected interatomic distances (in Å) and angles (in °) in **4**.

Symmetry operations: I 1-x,-Y,1-z

Bi1 Cl2^{I}	2.6818(12)	Cl3 Bi1 Cl2	86.01(4)	N4 Bi1 Cl2	90.0
Bi1 Cl2	2.6818(12)	Cl3^{I} Bi1 Cl2^{I}	86.01(4)	N4 Bi1 Cl3	90.0
Bi1 Cl3^{I}	2.6778(11)	Cl3^{I} Bi1 Cl2	93.99(4)	N4 Bi1 Cl3^{I}	90.0
Bi1 Cl3	2.6778(11)	Cl3 Bi1 Cl2^{I}	93.99(4)	N4I Bi1 Cl3^{I}	90.0
Bi1 N4	2.575(5)	Cl3^{I} Bi1 Cl3	180.0	N4^{I} Bi1 Cl3	90.0
Bi1 N4^{I}	2.575(5)	N4 Bi1 Cl2^{I}	90.0	N4^{I} Bi1 N4	180.0
		N4^{I} Bi1 Cl2	90.0		
Cl2^{I} Bi1 Cl2	180.0	N4^{I} Bi1 Cl2^{I}	90.0		

Crystallographic details for 5

Table S11: Crystallographic data for **5**.

	5
Empirical formula	$C_{25}H_{21}BiCl_4N_5$
Formula weight /g·mol^{-1}	742.25
Crystal colour and shape	colourless block
Crystal size	0.15 × 0.12 × 0.09
Crystal system	triclinic
Space group	$P\bar{1}$
a /Å	8.7574(7)
b /Å	11.1147(9)
c /Å	14.6158(12)
α /°	82.7440(10)
β /°	78.5740(10)
γ /°	70.6280(10)
V /Å^3	1312.67(18)
Z	2
ρ_{calc} /g·cm^{-3}	1.878
μ(Mo$_{K\alpha}$) /mm^{-1}	7.147
measurement temp. /K	100
Absorption correction type	multi-scan
Min/max transmission	0.5810/0.7460
2Θ range /°	2.848-60.24
No. of measured reflections	19881
No. of independent reflections	7664
R(int)	0.0747
No. of indep. reflections ($I > 2\sigma(I)$)	6915
No. of parameters	352
R_1 ($I > 2\sigma(I)$)	0.0345
wR_2 (all data)	0.1057
S (all data)	0.768
$\Delta\rho_{max}$, $\Delta\rho_{min}$ /e· Å^{-3}	2.86/-1.37

Details of crystal structure refinement: A minor disorder in the bridging *bipy* unit was modeled with four half occupied positions in the pyridyl moiety. The hydrogen atoms attached to N3 and N4 have half occupancy to correctly model the N-H···N-hydrogen bridges between *bipy* units.

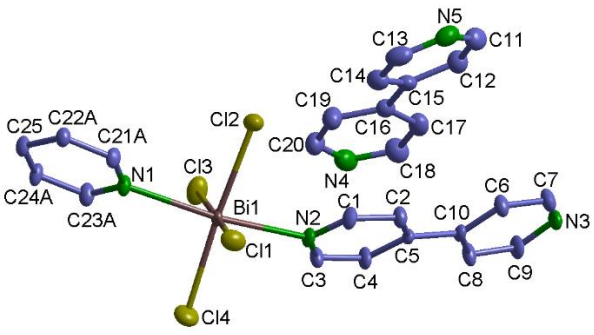

Figure S6: Asymmetric unit of **5**, ellipsoids at 50% probability.

Table S12: Selected interatomic distances (in Å) and angles (in °) in **5**.

Bi1 Cl4	2.6665(13)	Cl4 Bi1 Cl3	90.96(5)	N2 Bi1 Cl1	96.23(10)
Bi1 Cl2	2.6709(12)	Cl4 Bi1 Cl1	90.68(4)	N2 Bi1 N1	169.40(13)
Bi1 Cl3	2.6860(14)	Cl3 Bi1 Cl2	92.45(4)	N1 Bi1 Cl4	93.46(10)
Bi1 Cl1	2.6619(13)	Cl1 Bi1 Cl2	86.05(4)	N1 Bi1 Cl2	89.78(10)
Bi1 N2	2.523(3)	Cl1 Bi1 Cl3	175.53(4)	N1 Bi1 Cl3	84.31(10)
Bi1 N1	2.545(3)	N2 Bi1 Cl4	91.52(10)	N1 Bi1 Cl1	93.08(10)
		N2 Bi1 Cl2	85.81(10)		
Cl4 Bi1 Cl2	175.52(4)	N2 Bi1 Cl3	86.25(10)		

Crystallographic details for 6

Table S13: Crystallographic data for **6**.

	6
Empirical formula	$C_{40}H_{38}Cl_8N_8Sm_2$
Formula weight /g·mol^{-1}	1215.08
Crystal colour and shape	colourless block
Crystal size	0.23 × 0.15 × 0.05
Crystal system	monoclinic
Space group	*C*2/*m*
a /Å	13.205(4)
b /Å	12.340(4)
c /Å	8.1926(16)
α /°	90
β /°	121.97(3)
γ /°	90
V /Å^3	1132.5(6)
Z	1
ρ_{calc} /g·cm^{-3}	1.782
μ(Mo$_{K\alpha}$) /mm^{-1}	3.079
measurement temp. /K	100
Absorption correction type	multi-scan
Min/max transmission	0.5679/0.7455
2Θ range /°	4.912-54.072
No. of measured reflections	6951
No. of independent reflections	1312
R(int)	0.0207
No. of indep. reflections ($I > 2\sigma(I)$)	1310
No. of parameters	73
R_1 ($I > 2\sigma(I)$)	0.0157
wR_2 (all data)	0.0406
S (all data)	1.120
$\Delta\rho_{max}$, $\Delta\rho_{min}$ /e· Å^{-3}	1.17/-0.23

Details of crystal structure refinement: The hydrogen atom attached to N2 has half occupancy to correctly model the pyridine·pyridinium homodimer.

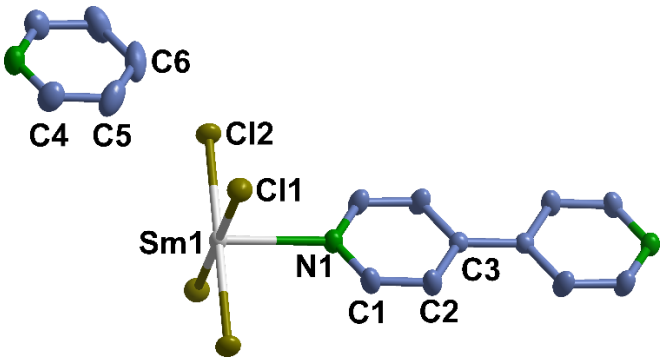

Figure S7: Asymmetric unit of **6**, ellipsoids at 50% probability.

Table S14: Selected interatomic distances (in Å) and angles (in °) in **6**.

Symmetry operations: I 1-x, 1-y, -z

Sm1 Cl1	2.6616(10)	Cl1 Sm1 $Cl2^{I}$	86.49(4)	$N1^{I}$ Sm1 Cl1	90.0
Sm1 $Cl1^{I}$	2.6616(10)	$Cl1^{I}$ Sm1 $Cl2^{I}$	93.51(4)	N1 Sm1 Cl2	90.0
Sm1 Cl2	2.6631(13)	Cl1 Sm1 Cl2	93.51(3)	$N1^{I}$ Sm1 Cl2	90.0
Sm1 $Cl2^{I}$	2.6631(13)	$Cl1^{I}$ Sm1 Cl2	86.49(4)	$N1^{I}$ Sm1 $Cl2^{I}$	90.0
Sm1 $N1^{I}$	2.592(2)	Cl2 Sm1 $Cl2^{I}$	180.0	N1 Sm1 $Cl2^{I}$	90.0
Sm1 N1	2.592(2)	N1 Sm1 Cl1	90.0	$N1^{I}$ Sm1 N1	180.0
		$N1^{I}$ Sm1 $Cl1^{I}$	90.0		
Cl1 Sm1 $Cl1^{I}$	180.00(2)	N1 Sm1 $Cl1^{I}$	90.0		

Crystallographic details for 7

Table S15: Crystallographic data for **7**.

	7
Empirical formula	$C_{20}H_{19}Cl_4N_4Tb$
Formula weight /g·mol^{-1}	616.11
Crystal colour and shape	colourless block
Crystal size	0.339 × 0.321 × 0.200
Crystal system	monoclinic
Space group	*C*2/*c*
a /Å	14.5387(4)
b /Å	12.2326(3)
c /Å	13.1136(4)
α /°	90
β /°	107.7010(10)
γ /°	90
V /Å^3	2221.79(11)
Z	4
ρ_{calc} /g·cm^{-3}	1.842
μ(Mo$_{K\alpha}$) /mm^{-1}	3.679
measurement temp. /K	173.15
Absorption correction type	multi-scan
Min/max transmission	0.6508/0.7460
2Θ range /°	4.442-60.148
No. of measured reflections	17699
No. of independent reflections	3180
R(int)	0.0278
No. of indep. reflections ($I > 2\sigma(I)$)	2998
No. of parameters	134
R_1 ($I > 2\sigma(I)$)	0.0169
wR_2 (all data)	0.0425
S (all data)	1.094
$\Delta\rho_{max}$, $\Delta\rho_{min}$ /e· Å^{-3}	0.56/-0.91

Details of crystal structure refinement: The hydrogen atom attached to N3 has half occupancy to correctly model the pyridine·pyridinium homodimer.

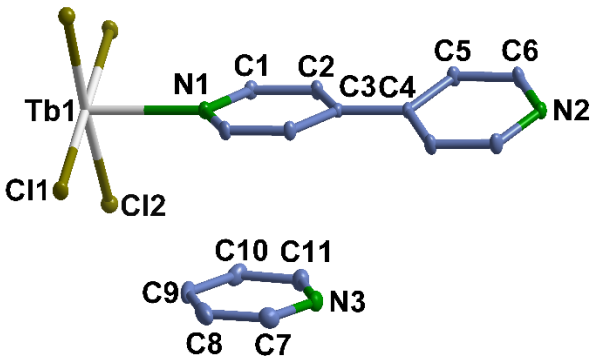

Figure S8: Asymmetric unit of **7**, ellipsoids at 50% probability.

Table S16: Selected interatomic distances (in Å) and angles (in °) in **7**.

Symmetry operations: I 1-x,+y,1/2-z II 2+x,1+y,+z

Tb1 Cl1	2.6268(4)	$Cl2^{I}$ Tb1 Cl1	86.786(14)	N1 Tb1 $Cl2^{I}$	88.698(9)
Tb1 $Cl1^{I}$	2.6267(4)	$Cl2^{I}$ Tb1 $Cl1^{I}$	93.213(14)	N1 Tb1 $N2^{II}$	180.0
Tb1 $Cl2^{I}$	2.6224(4)	Cl2 Tb1 $Cl1^{I}$	86.786(14)	$N2^{II}$ Tb1 $Cl1^{I}$	90.033(9)
Tb1 Cl2	2.6225(4)	Cl2 Tb1 Cl1	93.213(14)	$N2^{II}$ Tb1 Cl1	90.032(9)
Tb1 N1	2.537(2)	$Cl2^{I}$ Tb1 Cl2	177.394(19)	$N2^{II}$ Tb1 $Cl2^{I}$	91.302(9)
Tb1 $N2^{II}$	2.542(2)	N1 Tb1 $Cl1^{I}$	89.967(9)	$N2^{II}$ Tb1 Cl2	91.303(9)
		N1 Tb1 Cl1	89.968(9)		
$Cl1^{I}$ Tb1 Cl1	179.936(18)	N1 Tb1 Cl2	88.697(9)		

Crystallographic details for 8

Table S17: Crystallographic data for **8**.

	8
Empirical formula	$C_{20}H_{19}Cl_4LuN_4$
Formula weight /g·mol^{-1}	632.16
Crystal colour and shape	colourless block
Crystal size	0.16 × 0.11 × 0.10
Crystal system	monoclinic
Space group	*C*2/*c*
a /Å	14.516(3)
b /Å	12.071(2)
c /Å	13.240(3)
α /°	90
β /°	105.64(3)
γ /°	90
V /Å^3	2234.1(8)
Z	4
ρ_{calc} /g·cm^{-3}	1.880
μ(Mo$_{K\alpha}$) /mm^{-1}	4.912
measurement temp. /K	100
Absorption correction type	multi-scan
Min/max transmission	0.4478/0.7455
2Θ range /°	4.458-54.078
No. of measured reflections	13338
No. of independent reflections	2454
R(int)	0.0253
No. of indep. reflections ($I > 2\sigma(I)$)	2395
No. of parameters	134
R_1 ($I > 2\sigma(I)$)	0.0177
wR_2 (all data)	0.0424
S (all data)	1.158
$\Delta\rho_{max}$, $\Delta\rho_{min}$ /e· Å^{-3}	1.54/-0.33

Details of crystal structure refinement: The hydrogen atom attached to N3 has half occupancy to correctly model the pyridine·pyridinium homodimer.

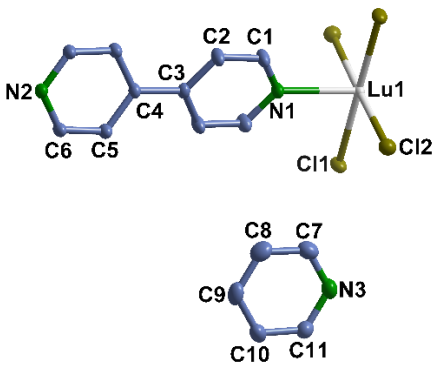

Figure S9: Asymmetric unit of **8**, ellipsoids at 50% probability.

Table S18: Selected interatomic distances (in Å) and angles (in °) in **8**.

Symmetry operations: I -X,+Y,1/2-Z II +X,-1+Y,+Z

Lu1 $Cl1^{I}$	2.5675(8)	$Cl2^{I}$ Lu1 $Cl1^{I}$	87.91(4)	N1 Lu1 $Cl2^{I}$	90.835(14)
Lu1 Cl1	2.5675(8)	$Cl2^{I}$ Lu1 Cl1	92.09(4)	N1 Lu1 $N2^{II}$	180.0
Lu1 $Cl2^{I}$	2.5576(9)	Cl2 Lu1 Cl1	87.91(4)	$N2^{II}$ Lu1 Cl1	89.773(13)
Lu1 Cl2	2.5577(9)	Cl2 Lu1 $Cl1^{I}$	92.09(4)	$N2^{II}$ Lu1 $Cl1^{I}$	89.774(13)
Lu1 N1	2.453(3)	$Cl2^{I}$ Lu1 Cl2	178.33(3)	$N2^{II}$ Lu1 $Cl2^{I}$	89.165(14)
Lu1 $N2^{II}$	2.468(3)	N1 Lu1 Cl1	90.227(13)	$N2^{II}$ Lu1 Cl2	89.164(14)
		N1 Lu1 $Cl1^{I}$	90.226(12)		
Cl1 Lu1 $Cl1^{I}$	179.55(2)	N1 Lu1 Cl2	90.836(14)		

Crystallographic details for 9

Table S19: Crystallographic data for **9**.

	9
Empirical formula	$C_{60}H_{52}Cl_8N_{12}Sm_2$
Formula weight /g·mol^{-1}	1525.43
Crystal colour and shape	colourless block
Crystal size	0.433 × 0.276 × 0.189
Crystal system	monoclinic
Space group	$P2_1/c$
a /Å	8.7594(4)
b /Å	20.0090(9)
c /Å	17.2945(8)
α /°	90
β /°	92.8550(10)
γ /°	90
V /Å^3	3027.4(2)
Z	2
ρ_{calc} /g·cm^{-3}	1.673
μ(Mo$_{K\alpha}$) /mm^{-1}	2.324
measurement temp. /K	100
Absorption correction type	multi-scan
Min/max transmission	0.6174/0.7460
2Θ range /°	3.114-60.172
No. of measured reflections	48005
No. of independent reflections	8676
R(int)	0.0653
No. of indep. reflections ($I > 2\sigma(I)$)	6477
No. of parameters	478
R_1 ($I > 2\sigma(I)$)	0.0334
wR_2 (all data)	0.0601
S (all data)	1.009
$\Delta\rho_{max}$, $\Delta\rho_{min}$ /e· Å^{-3}	0.76/-1.75

Details of crystal structure refinement: The hydrogen atom attached to N4 was refined to have a half occupancy to correctly model the pyridinium·*bipy* heterodimer. A disorder in the *bipy* unit within this dimer was modeled by half occupied positions for all C/N-atoms.

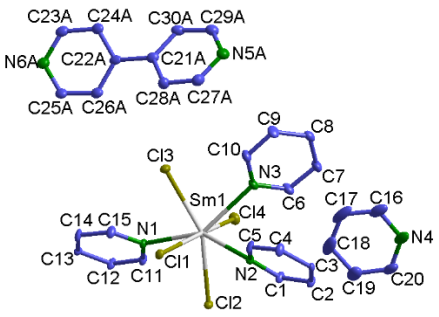

Figure S10: Asymmetric unit of **9**, ellipsoids at 50% probability.

Table S20: Selected interatomic distances (in Å) and angles (in °) in **9**.

Sm1 Cl3	2.7031(7)	Cl4 Sm1 Cl2	84.52(2)	N3 Sm1 Cl3	75.66(6)
Sm1 Cl4	2.6792(7)	Cl4 Sm1 Cl1	168.40(2)	N3 Sm1 Cl4	79.36(5)
Sm1 Cl2	2.7311(7)	Cl1 Sm1 Cl3	83.88(2)	N3 Sm1 Cl2	130.44(6)
Sm1 Cl1	2.6882(7)	Cl1 Sm1 Cl2	89.18(2)	N3 Sm1 Cl1	112.04(5)
Sm1 N2	2.587(2)	N2 Sm1 Cl3	126.96(5)	N1 Sm1 Cl3	76.62(5)
Sm1 N3	2.675(2)	N2 Sm1 Cl4	109.62(5)	N1 Sm1 Cl4	85.15(5)
Sm1 N1	2.592(2)	N2 Sm1 Cl2	76.06(5)	N1 Sm1 Cl2	77.09(5)
		N2 Sm1 Cl1	78.10(5)	N1 Sm1 Cl1	83.96(5)
Cl3 Sm1 Cl2	153.36(2)	N2 Sm1 N3	66.24(8)	N1 Sm1 N3	146.01(7)
Cl4 Sm1 Cl3	97.45(2)	N2 Sm1 N1	147.73(8)		

Crystallographic details for 10

Table S21: Crystallographic data for **10**.

	10
Empirical formula	$C_{30}H_{26}Cl_4N_6Pr$
Formula weight /g·mol^{-1}	753.28
Crystal colour and shape	colourless plate
Crystal size	0.06 × 0.01 × 0.01
Crystal system	monoclinic
Space group	$P2_1/c$
a /Å	8.8374(18)
b /Å	20.136(4)
c /Å	17.364(4)
α /°	90
β /°	92.75(3)
γ /°	90
V /Å^3	3086.4(11)
Z	4
ρ_{calc} /g·cm^{-3}	1.621
μ(Mo$_{K\alpha}$) /mm^{-1}	1.956
measurement temp. /K	173(2)
Absorption correction type	multi-scan
Min/max transmission	0.6119/0.7455
2Θ range /°	3.1-54.32
No. of measured reflections	37589
No. of independent reflections	6808
R(int)	0.0988
No. of indep. reflections ($I > 2\sigma(I)$)	4813
No. of parameters	554
R_1 ($I > 2\sigma(I)$)	0.0443
wR_2 (all data)	0.0823
S (all data)	1.010
$\Delta\rho_{max}$, $\Delta\rho_{min}$ /e· Å^{-3}	0.94/-0.49

Details of crystal structure refinement: The hydrogen atom attached to N4 was refined to have a half occupancy to correctly model the pyridinium·*bipy* heterodimer. The disorder in the *bipy* molecules was modelled with half occupied positions for the C-atoms C21, 22, 24, 25, 26, 27, 29, 30 in the pyridyl moieties.

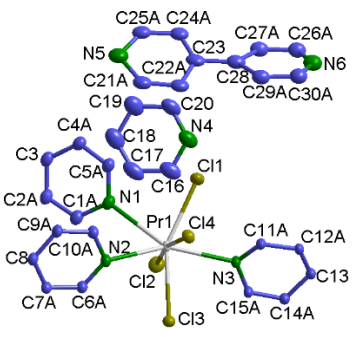

Figure S11: Asymmetric unit of **10**, ellipsoids at 50% probability.

Table S22: Selected interatomic distances (in Å) and angles (in °) in **10**.

Pr1 N3	2.638(3)	N2 Pr1 Cl2	109.79(8)	Cl2 Pr1 Cl1	98.01(4)
Pr1 N2	2.645(4)	N3 Pr1 N1	146.19(11)	N1 Pr1 Cl1	75.78(9)
Pr1 Cl2	2.7227(13)	N2 Pr1 N1	66.14(11)	Cl4 Pr1 Cl1	83.54(4)
Pr1 N1	2.727(4)	Cl2 Pr1 N1	79.32(9)	N3 Pr1 Cl3	77.08(8)
Pr1 Cl4	2.7287(12)	N3 Pr1 Cl4	84.24(8)	N2 Pr1 Cl3	76.13(8)
Pr1 Cl1	2.7428(13)	N2 Pr1 Cl4	77.66(8)	Cl2 Pr1 Cl3	84.34(4)
Pr1 Cl3	2.7718(12)	Cl2 Pr1 Cl4	168.61(4)	N1 Pr1 Cl3	130.14(9)
		N1 Pr1 Cl4	111.92(9)	Cl4 Pr1 Cl3	89.32(4)
N3 Pr1 N2	147.65(11)	N3 Pr1 Cl1	76.93(8)	Cl1 Pr1 Cl3	153.60(4)
N3 Pr1 Cl2	85.13(8)	N2 Pr1 Cl1	126.41(8)		

Table S23: Comparison of selected interatomic distances of compounds **1**-**10** with those of literature-known reference compounds.

Compound	M-X-bond length range / Å	M-N-bond length range / Å	Reference compound	M-X-bond length range / Å	M-N bond length range / Å
$^{1}_{\infty}[Bi_2Cl_6(bipy)_2]$ (**1a**)	2.514-2.905	2.515-2.539	$^{2}_{\infty}[Bi_2Cl_6(pyz)_4]$[1]	2.563-3.054	2.491-2.751
$^{1}_{\infty}[Bi_2Cl_6(bipy)_2]$ (**1b**)	2.503-2.941	2.467-2.576	See **1a**		
$^{1}_{\infty}[Bi_2Br_6(bipy)_2]$ (**2**)	2.644-3.078	2.454-2.592	Bi_2Br_6(2,2'-*bipy*)$_2$[2]	2.681-3.032	2.423-2.506
$^{1}_{\infty}[Bi_2I_6(bipy)_2]$ (**3**)	2.871-3.334	2.525-2.585	Bi_2I_6(3-methylpyridine)$_4$[3]	2.923-3.237	2.518-2.578
[H*py*·*py*]$^{1}_{\infty}[BiCl_4(bipy)]$ (**4**)	2.677-2.682	2.576	See **1a**		
[H*bipy*·*bipy*][(H*bipy*)$BiCl_4$(μ-*bipy*)$BiCl_4$(*bipy*)] (**5**)	2.661-2.685	2.523-2.546	See **1a**		
[H*py*·*py*]$^{1}_{\infty}[SmCl_4(bipy)]$ (**6**)	2.662-2.663	2.592	$^{2}_{\infty}[Sm_2Cl_6(bipy)_3]$·2*bipy*[4]	2.631-2.780	2.576-2.628
[H*py*·*py*]$^{1}_{\infty}[TbCl_4(bipy)]$ (**7**)	2.622-2.627	2.537-2.542	$[Tb_2Cl_6(bipy)(py)_6]$[5]	2.614-2.664	2.540-2.593
[H*py*·*py*]$^{1}_{\infty}[LuCl_4(bipy)]$ (**8**)	2.557-2.568	2.453-2.468	$^{1}_{\infty}[Lu_2Cl_5(bipy)_2(py)_4]$ $^{1}_{\infty}[LuCl_4(bipy)]$[6]	2.549-2.550[a]	2.391-2.400[a]
[H*py*·*bipy*]$_2$$^{2}_{\infty}[(SmCl_4)_2(bipy)_3]$ (**9**)	2.679-2.731	2.586-2.675	See **6**		
[H*py*·*bipy*]$_2$$^{2}_{\infty}[(PrCl_4)_2(bipy)_3]$ (**10**)	2.772-2.723	2.637-2.728	$^{2}_{\infty}[Pr_2Cl_6(bipy)_3]$·2*bipy*[4]	2.660-2.821	2.618-2.677

[a] within the anionic structure motif

Secondary Interactions in 1a

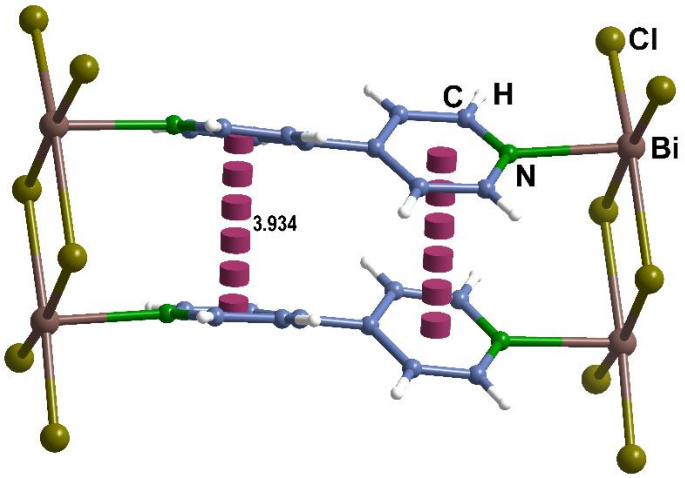

Figure S12: Offset-face-to-face π···π-interactions[7] in **1a**, with centroid-centroid distances of 3.934 Å.

Secondary Interactions in 1b-3

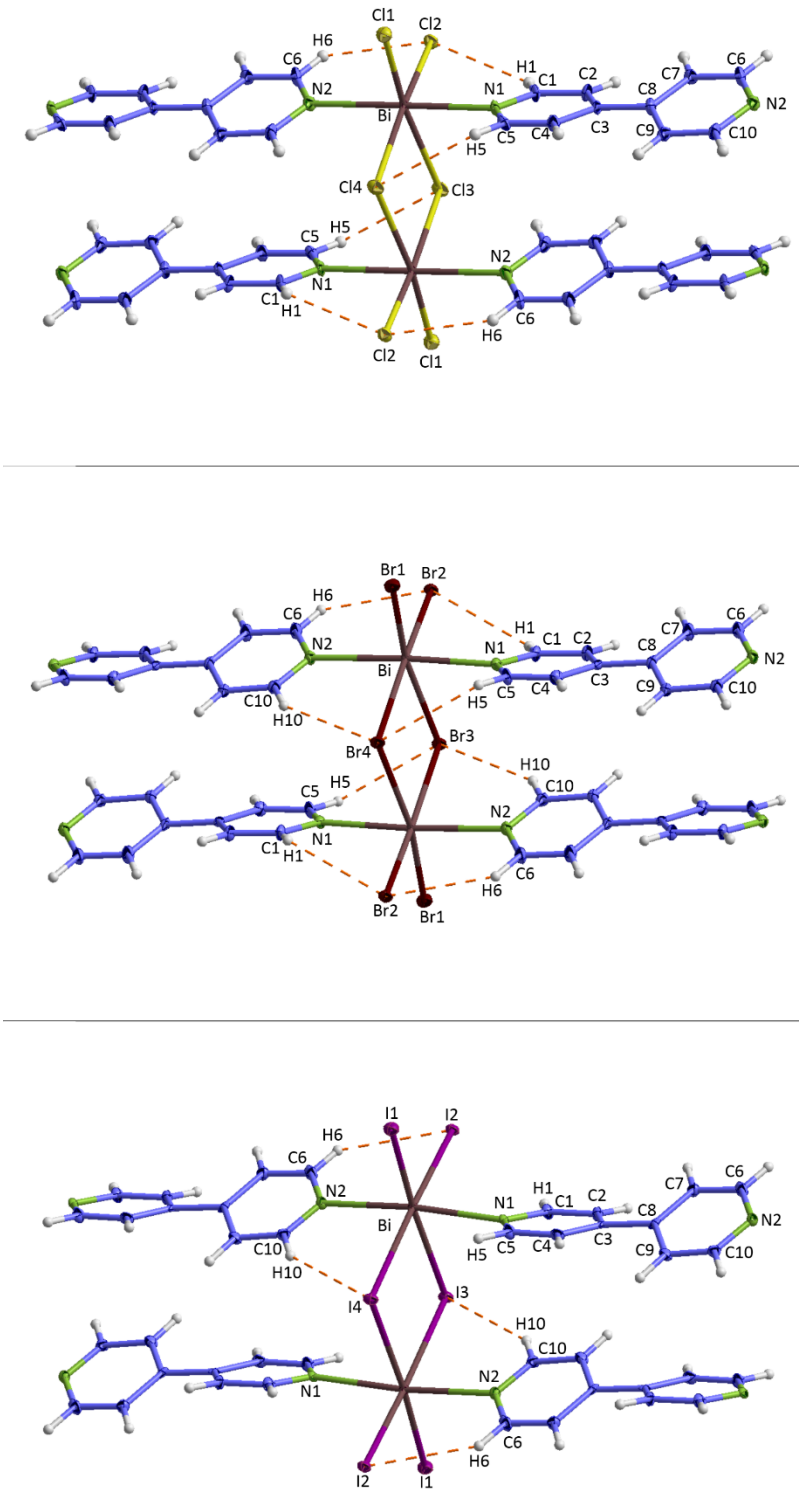

Figure S13: Hydrogen bonding in compounds **1b** (top), **2** (middle) and **3** (bottom). Hydrogen bonds are displayed as orange-dotted lines.

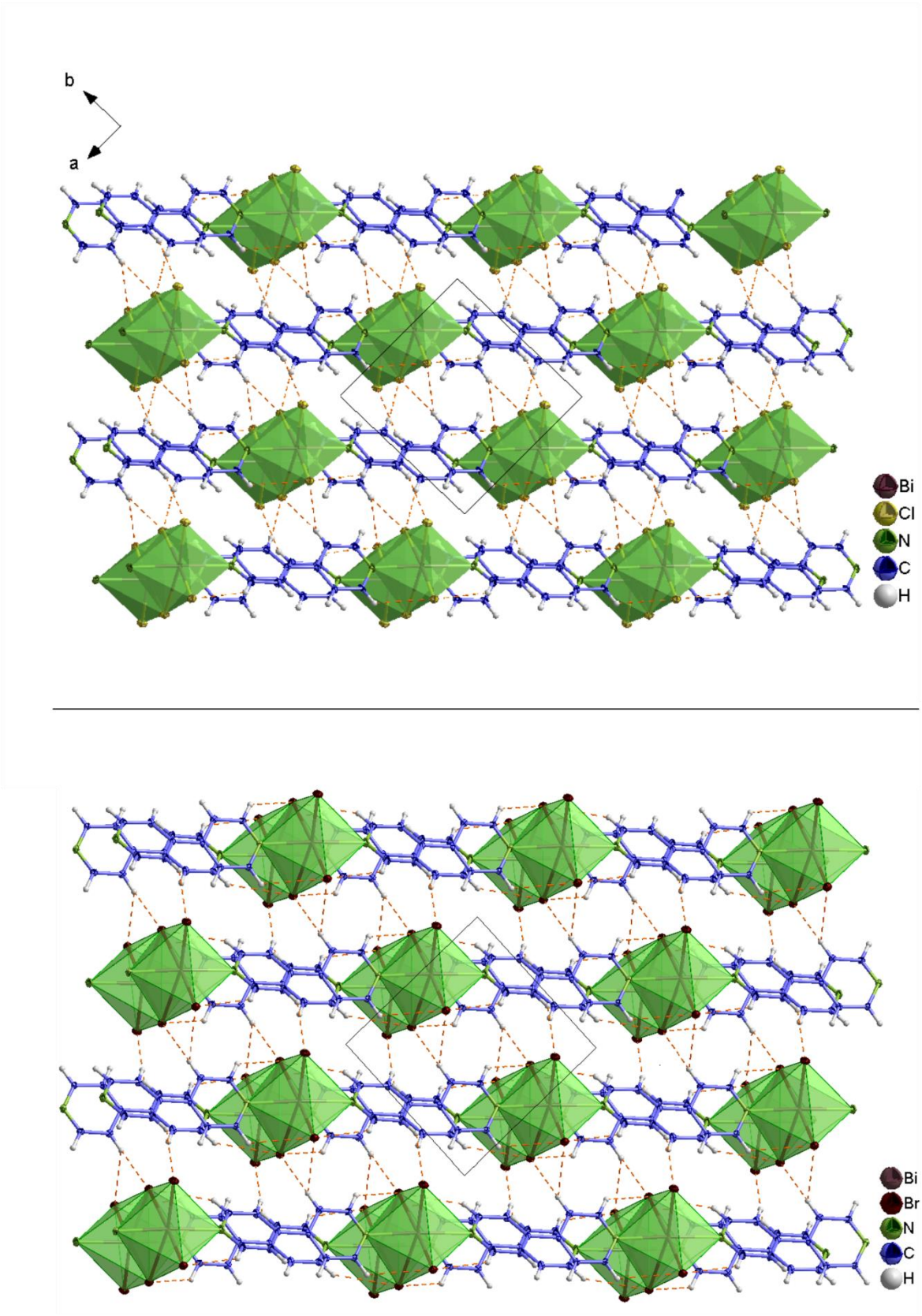

Figure S14: Additional Hydrogen bonding in compounds **1b** (top) and **2** (bottom). Hydrogen bonds are displayed as orange-dotted lines.

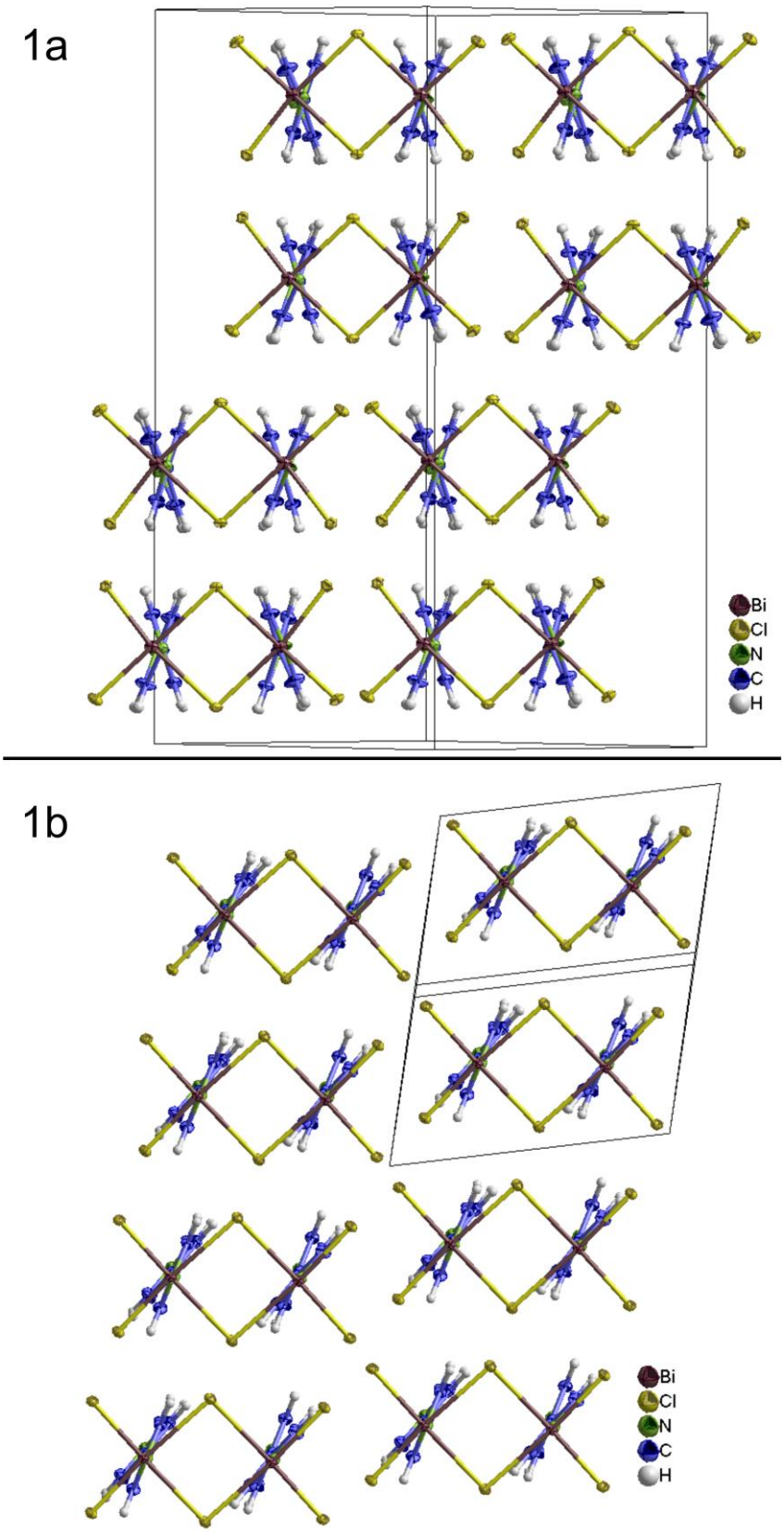

Figure S15. Fragment of the crystal structure of **1a**, view along [101] (top). Fragment of the crystal structure of **1b**, view along [110] (bottom).

Thermal analysis

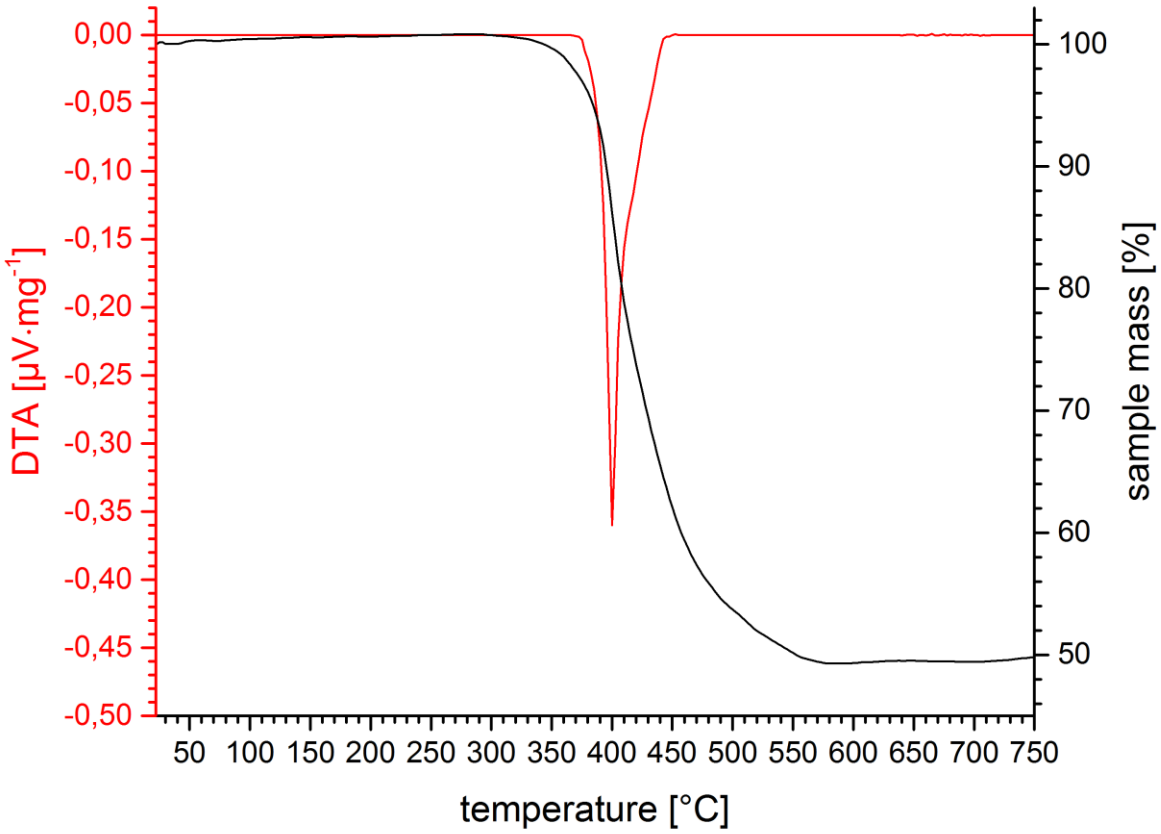

Figure S16. DTA- (red) and TG-curve (black) of α-$^{1}_{\infty}$[Bi_2Cl_6(*bipy*)$_2$] (**1a**).

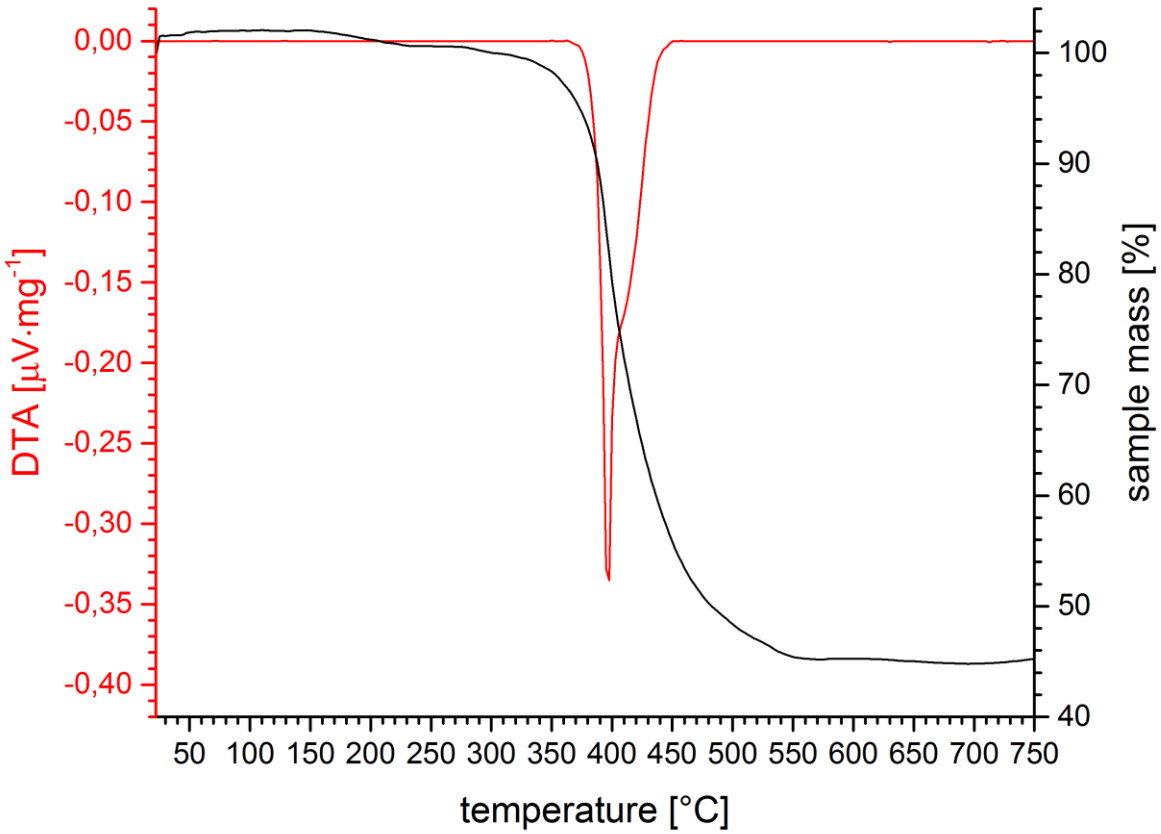

Figure S17. DTA- (red) and TG-curve (black) of β-$^{1}_{\infty}$[Bi_2Cl_6(*bipy*)$_2$] (**1b**).

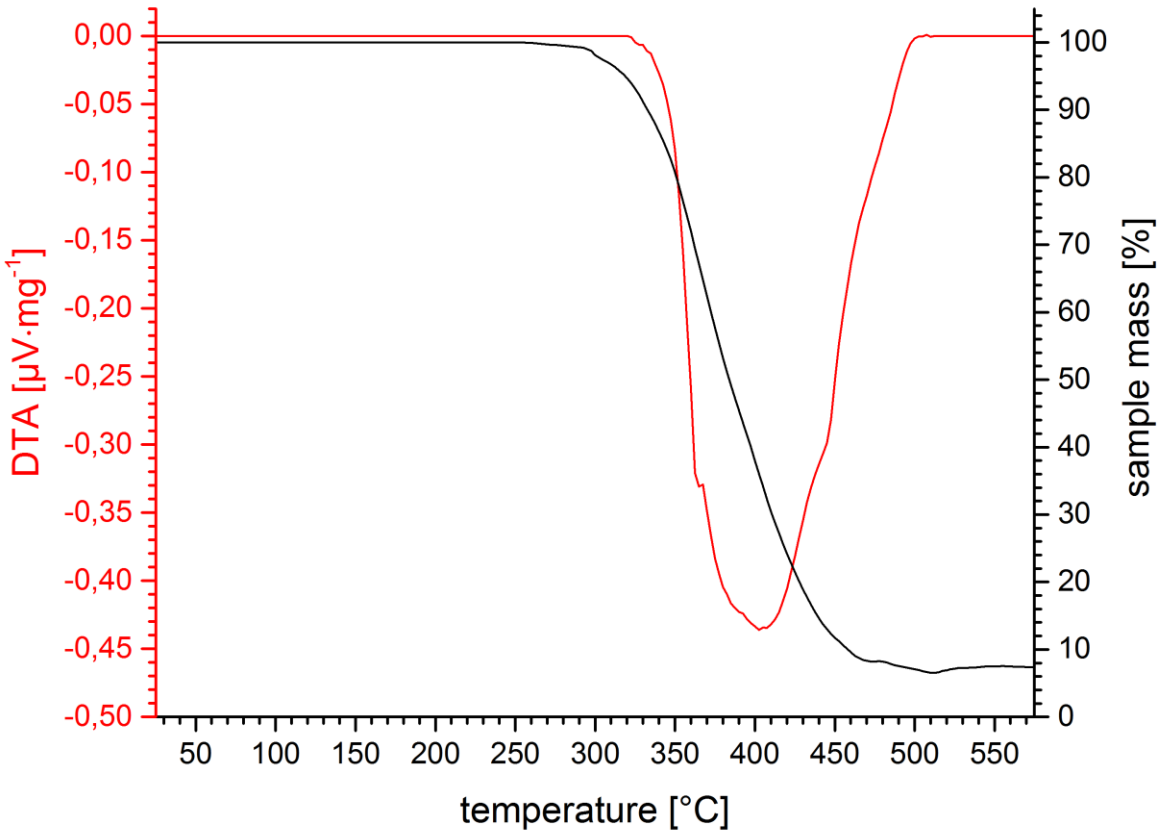

Figure S18. DTA- (red) and TG-curve (black) of $[Bi_2Br_6(bipy)_2]$ (**2**).

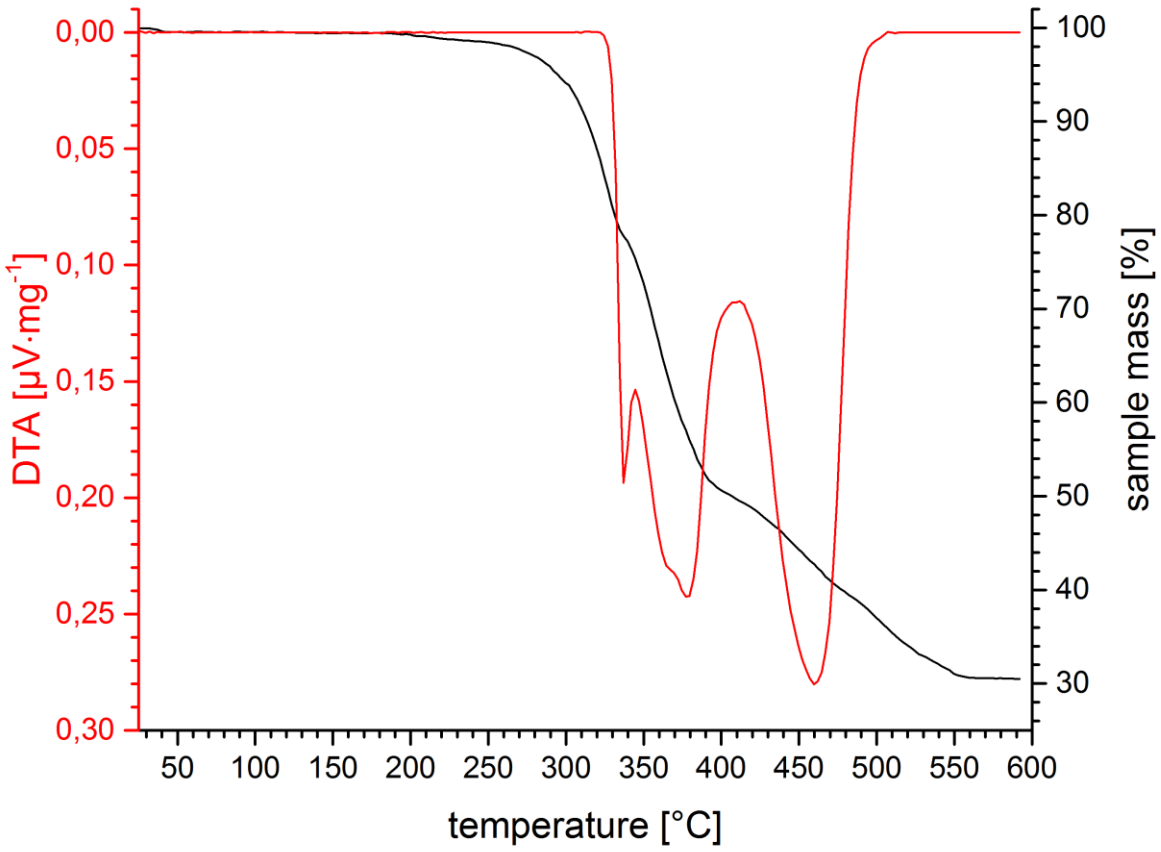

Figure S19. DTA- (red) and TG-curve (black) of $[Bi_2I_6(bipy)_2]$ (**3**).

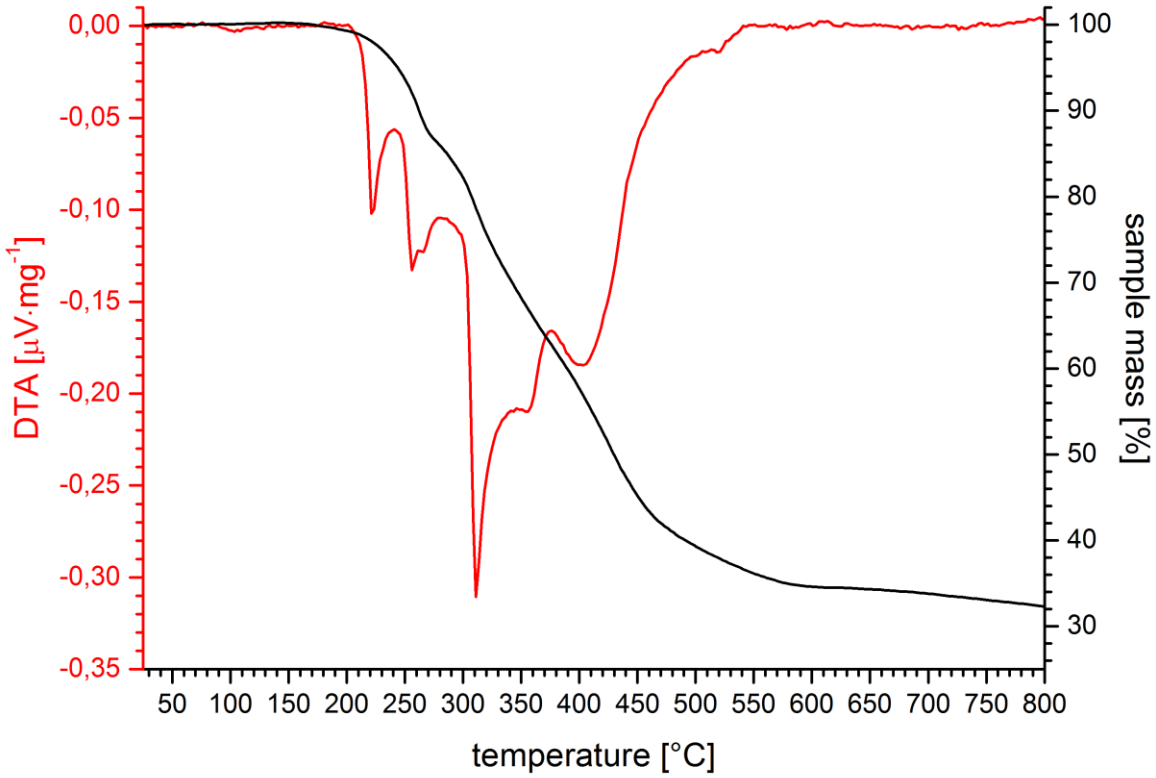

Figure S20. DTA- (red) and TG-curve (black) of [H*bipy*·*bipy*][(Hbipy)$BiCl_4$(µ-*bipy*)$BiCl_4$(*bipy*)] (**5**).

Powder diffraction

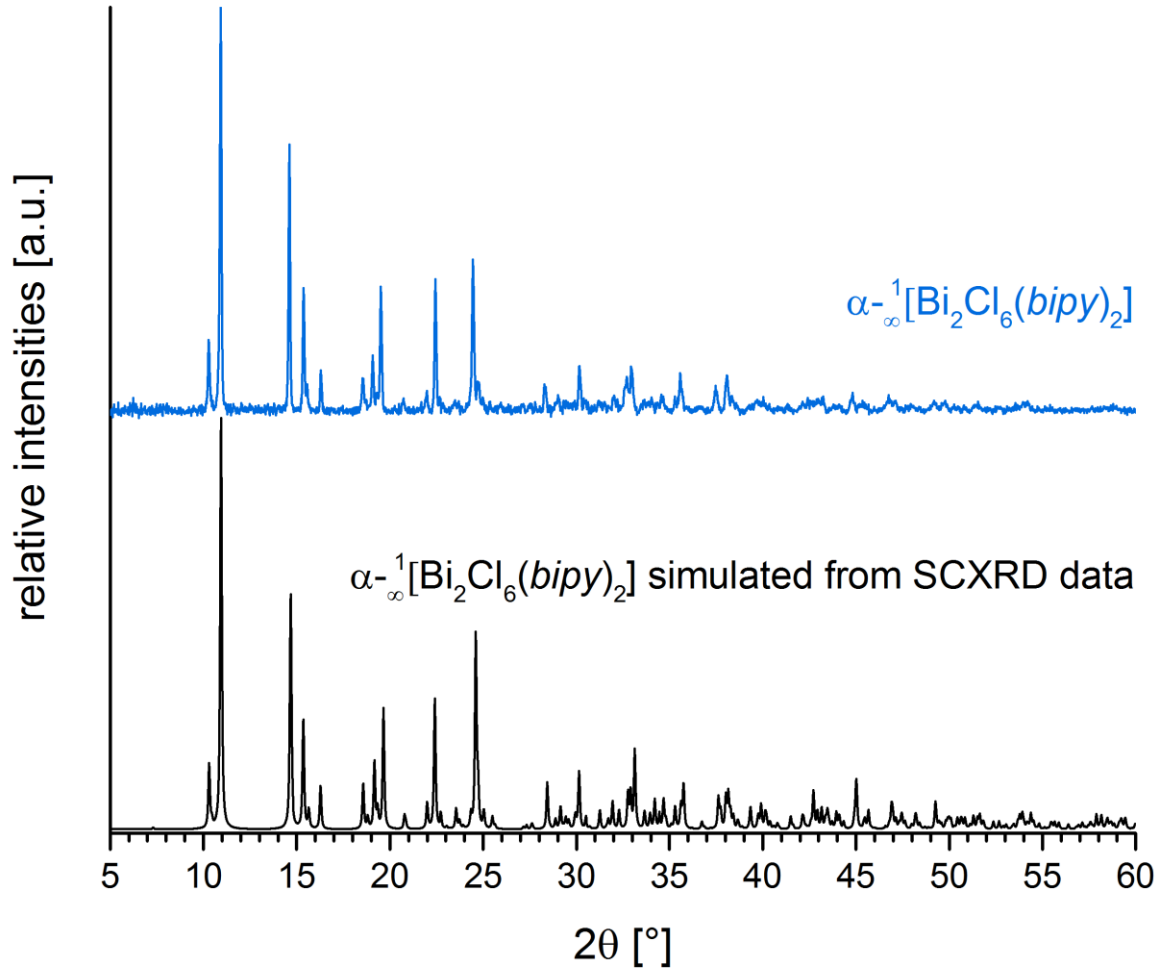

Figure S21. Comparison of the obtained powder pattern of α-$^{1}_{\infty}$[Bi_2Cl_6(*bipy*)$_2$] (**1a**) with a simulated diffractogram from SCXRD data illustrating the purity of the synthesized compound.

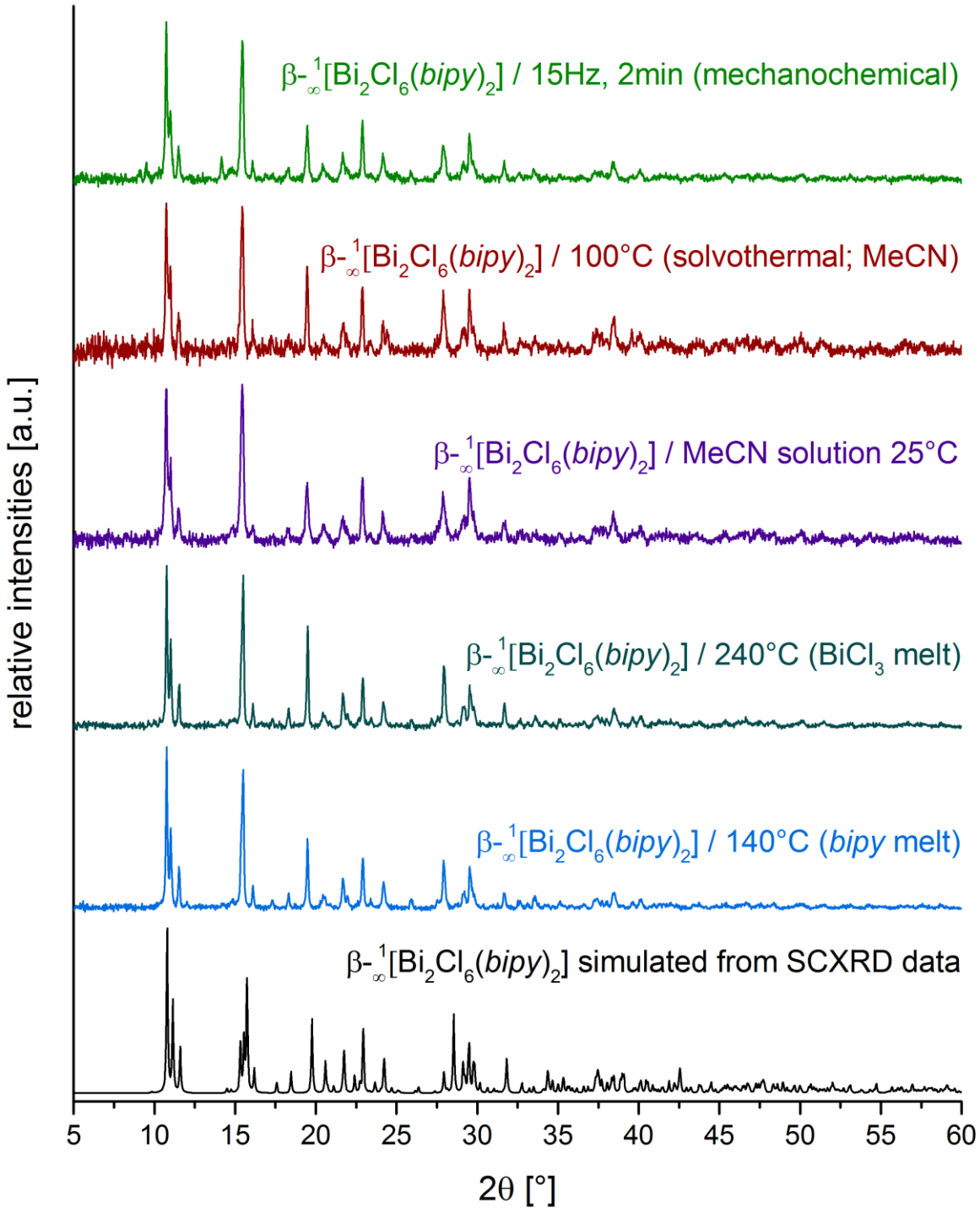

Figure S22. Comparison of the obtained powder patterns of β-$^{1}_{\infty}$[Bi$_2$Cl$_6$(*bipy*)$_2$] (**1b**) according to different synthesis methods with a simulated diffractogram from SCXRD data illustrating the purity of the synthesized compounds.

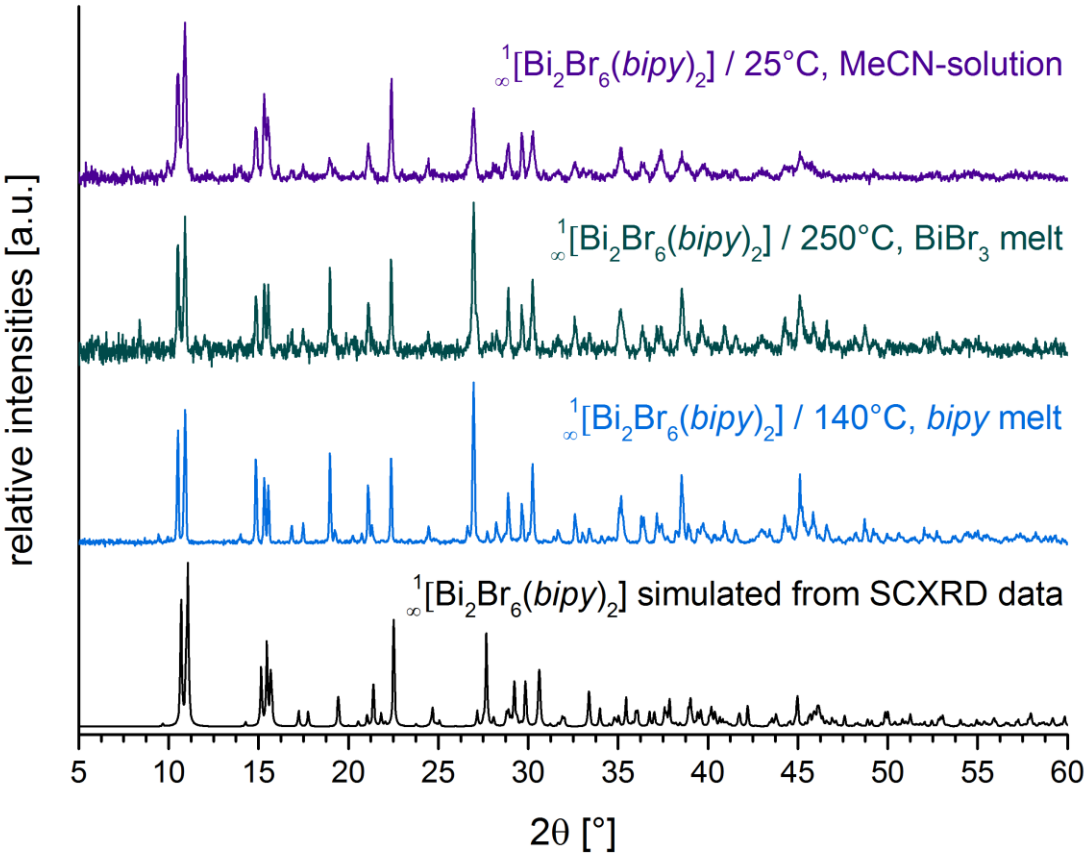

Figure S23. Comparison of the obtained powder patterns of $^1_\infty$[Bi$_2$Br$_6$(*bipy*)$_2$] (**2**) according to different synthesis methods with a simulated diffractogram from SCXRD data illustrating the purity of the synthesized compounds.

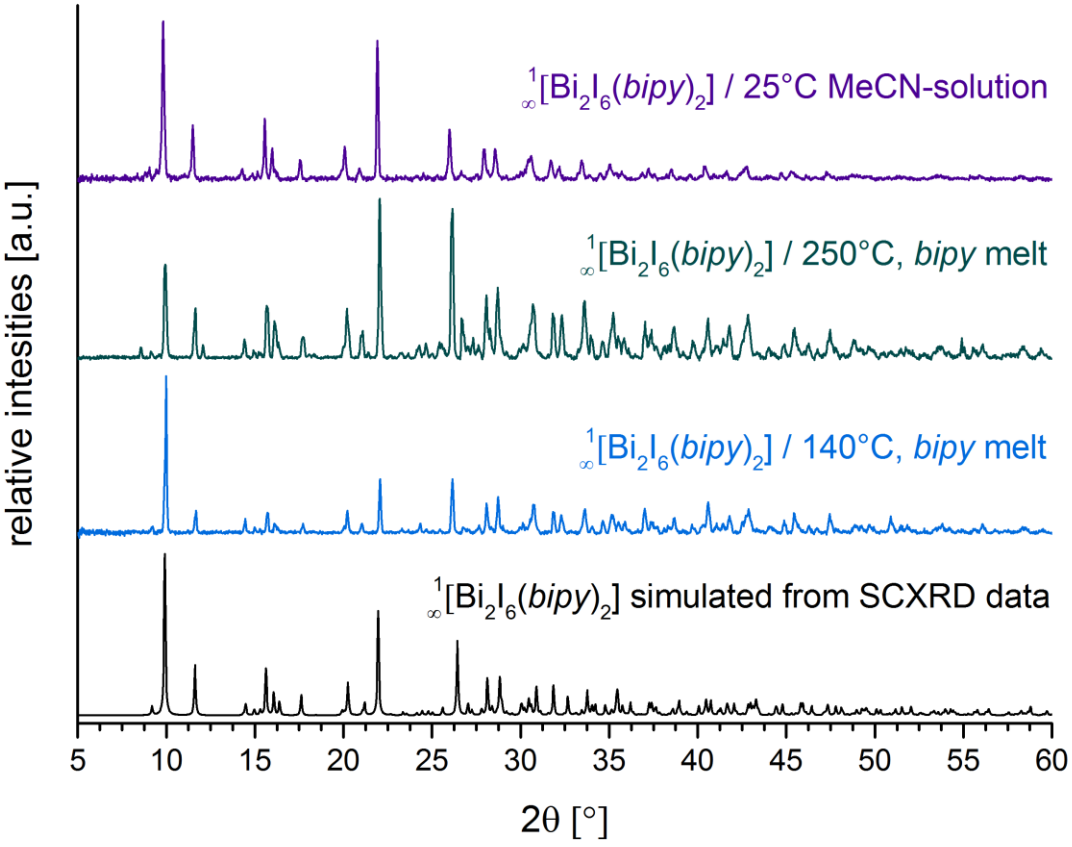

Figure S24. Comparison of the obtained powder patterns of $^{1}_{\infty}[Bi_2I_6(bipy)_2]$ (**3**) according to different synthesis methods with a simulated diffractogram from SCXRD data illustrating the purity of the synthesized compounds.

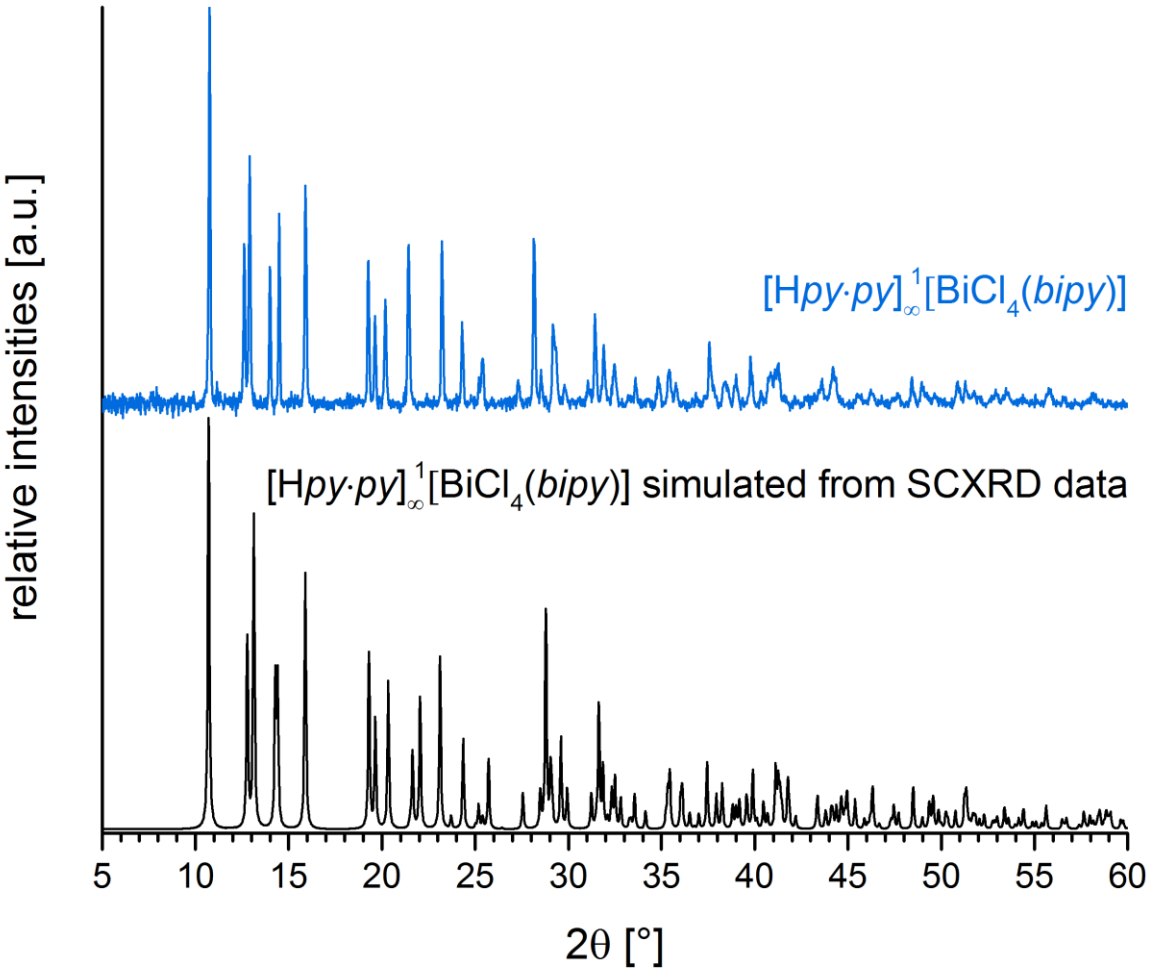

Figure S25. Comparison of the obtained powder pattern of [H*py·py*]$^{1}_{\infty}$[$BiCl_4$(*bipy*)] (**4**) with a simulated diffractogram from SCXRD data illustrating the purity of the synthesized compound.

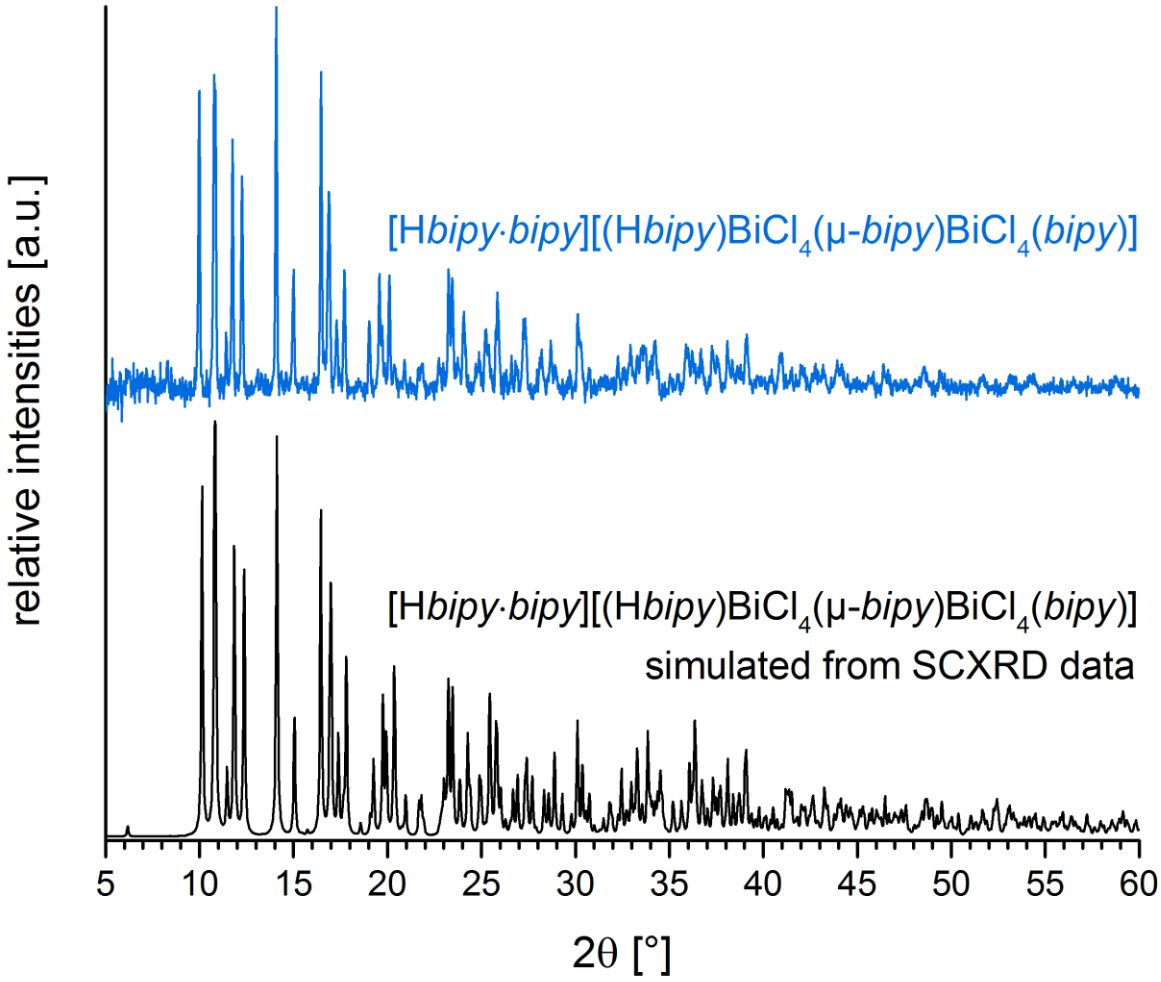

Figure S26. Comparison of the obtained powder pattern of [H*bipy*·*bipy*][(H*bipy*)$BiCl_4$(μ-*bipy*)$BiCl_4$(*bipy*)]Bi_2Cl_6(*bipy*)$_2$] (**5**) with a simulated diffractogram from SCXRD data illustrating the purity of the synthesized compound.

IR spectroscopy

α-$^1_\infty$[Bi_2Cl_6(*bipy*)$_2$] (**1a**): $\tilde{\nu}$= 3087 (w), 3051 (w), 1601 (s), 1530 (w), 1487 (w), 1415 (m), 1218 (m), 1067 (m), 1002 (m), 810 (s), 626 (s) cm^{-1}.

β-$^1_\infty$[Bi_2Cl_6(*bipy*)$_2$] (**1b**): $\tilde{\nu}$= 3090 (w), 3048 (w), 1602 (s), 1533 (m), 1489 (w), 1415 (s), 1331 (w), 1219 (s), 1067 (s), 1002 (s), 810 (s), 723 (m) cm^{-1}.

$^1_\infty$[Bi_2Br_6(*bipy*)$_2$] (**2**): $\tilde{\nu}$= 3089 (w), 3049 (w), 1600 (s), 1530 (m), 1486 (w), 1411 (s), 1326 (w), 1215 (s), 1065 (s), 1000 (s), 800 (s), 718 (m) cm^{-1}.

$^1_\infty$[Bi_2I_6(*bipy*)$_2$] (**3**): $\tilde{\nu}$= 1598 (m), 1521 (w), 1483 (w), 1407 (m), 1316 (w), 1212 (s), 1065 (s), 1001 (s), 800 (s), 719 (w) cm^{-1}.

[H*py*·*py*]$^1_\infty$[$BiCl_4$(*bipy*)] (**4**): $\tilde{\nu}$= 3083 (w), 3051 (w), 1598 (s), 1527 (w), 1488 (w), 1411 (m), 1220 (m), 1070 (m), 1000 (m), 806 (s), 625 (m) cm^{-1}.

[Hbi*py*·bi*py*][(Hbipy)$BiCl_4$(μ-*bipy*) $BiCl_4$(*bipy*)] (**5**): $\tilde{\nu}$= 3031 (w), 1596 (s), 1530 (w), 1489 (w), 1220 (m), 1067 (m), 995 (m), 823 (s), 759 (s), 695 (s), 622 (s) cm^{-1}.

Optical properties

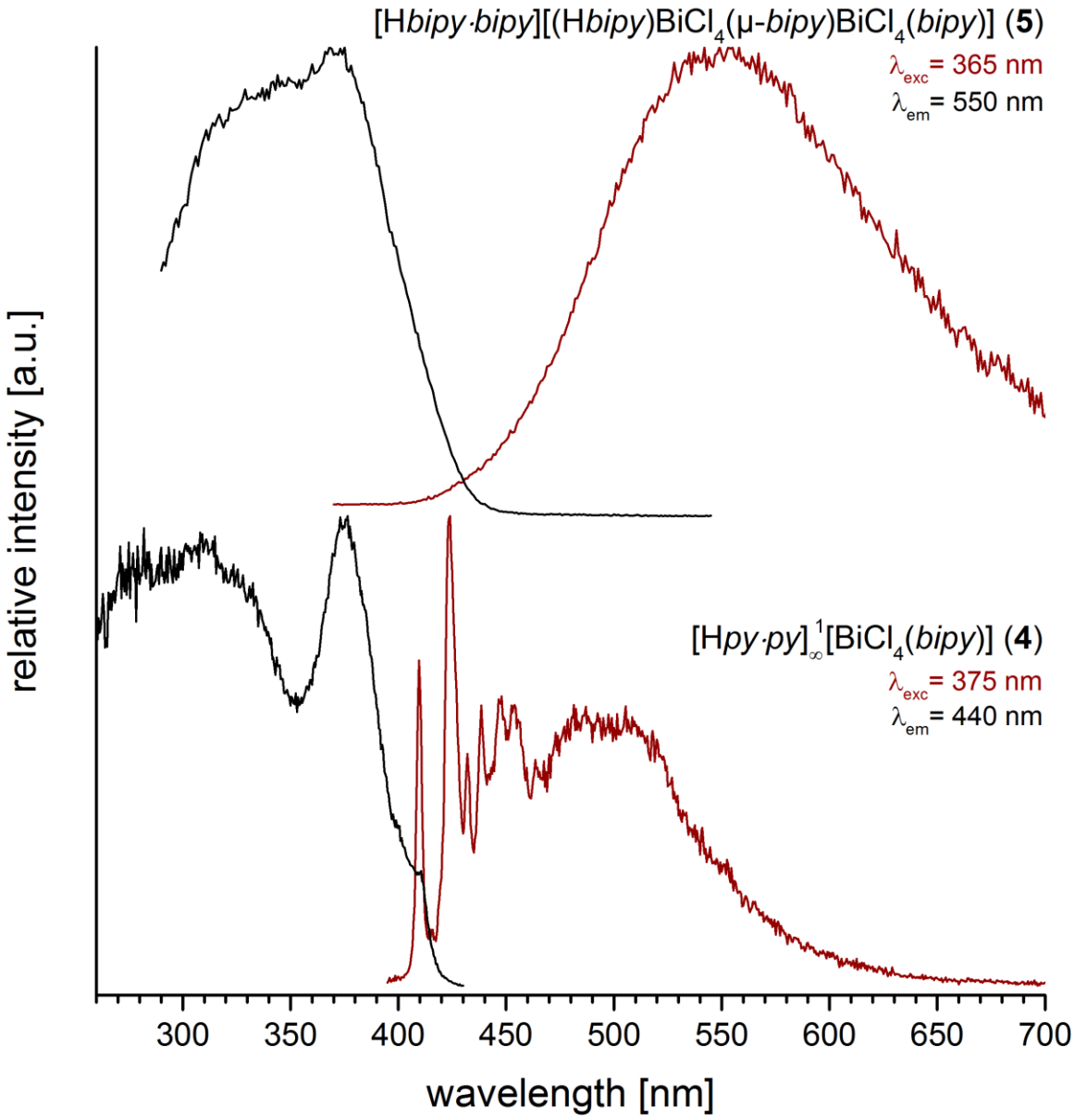

Figure S27. Excitation (black) and emission spectra (red) of $[Hpy{\cdot}py]^{1}_{\infty}[BiCl_4(bipy)]$ (**4**) and $[Hbipy{\cdot}bipy][(Hbipy)BiCl_4(\mu\text{-}bipy)BiCl_4(bipy)]Bi_2Cl_6(bipy)_2]$ (**5**) recorded at 77 K.

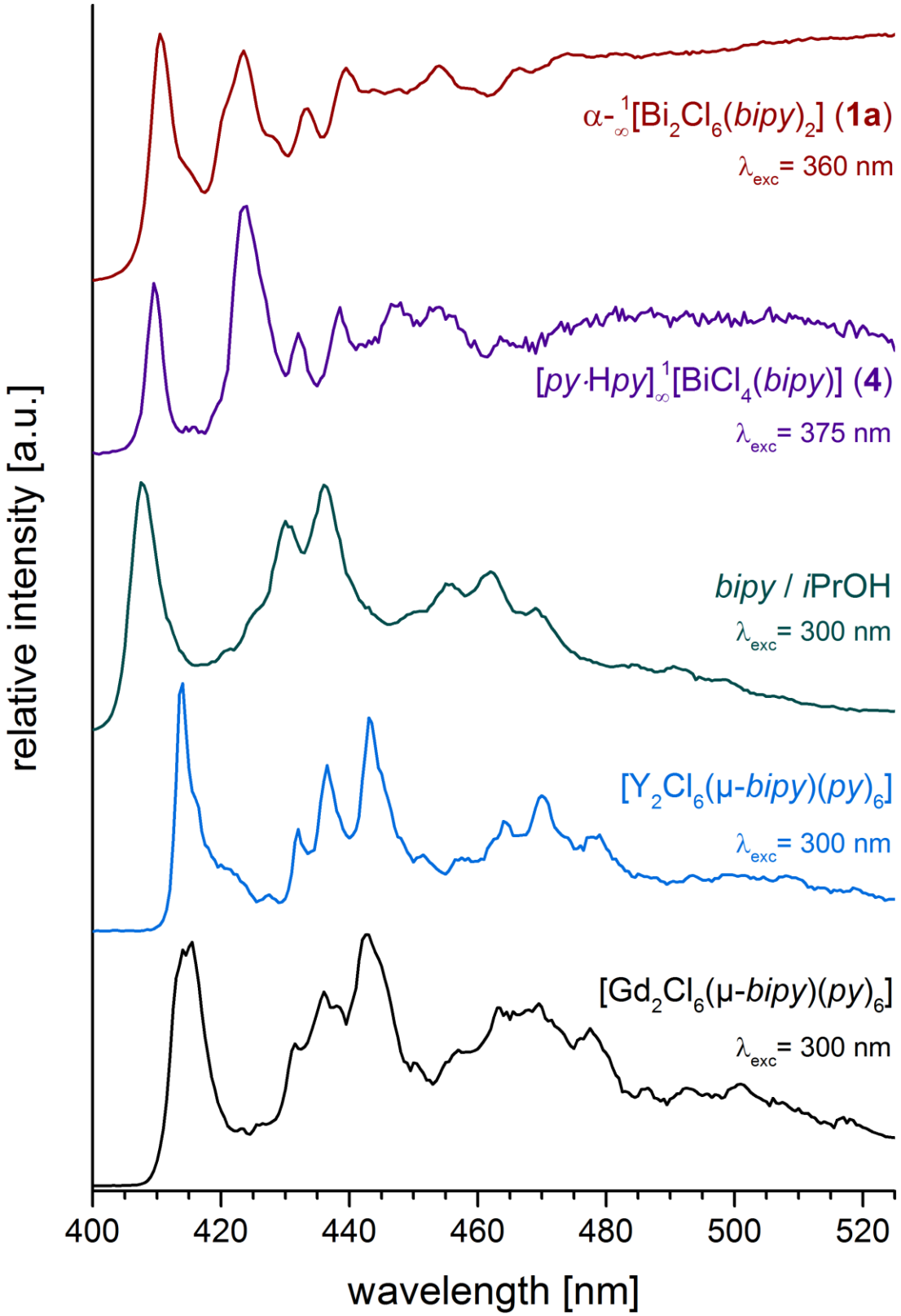

Figure S28. Comparison of the emission spectra of $[Gd_2Cl_6(\mu\text{-}bipy(py)_6$ (black), $[Y_2Cl_6(\mu\text{-}bipy(py)_6$ (blue), a *bipy*/*i*PrOH mixture (teal), $[Hpy{\cdot}py]^1_\infty[BiCl_4(bipy)]$ (**4**, violet) and $\alpha\text{-}^1_\infty[Bi_2Cl_6(bipy)_2]$ (**1a**, red) showing the $T_1 \rightarrow S_0$ transition of the organic ligand. All spectra were recorded at 77 K.

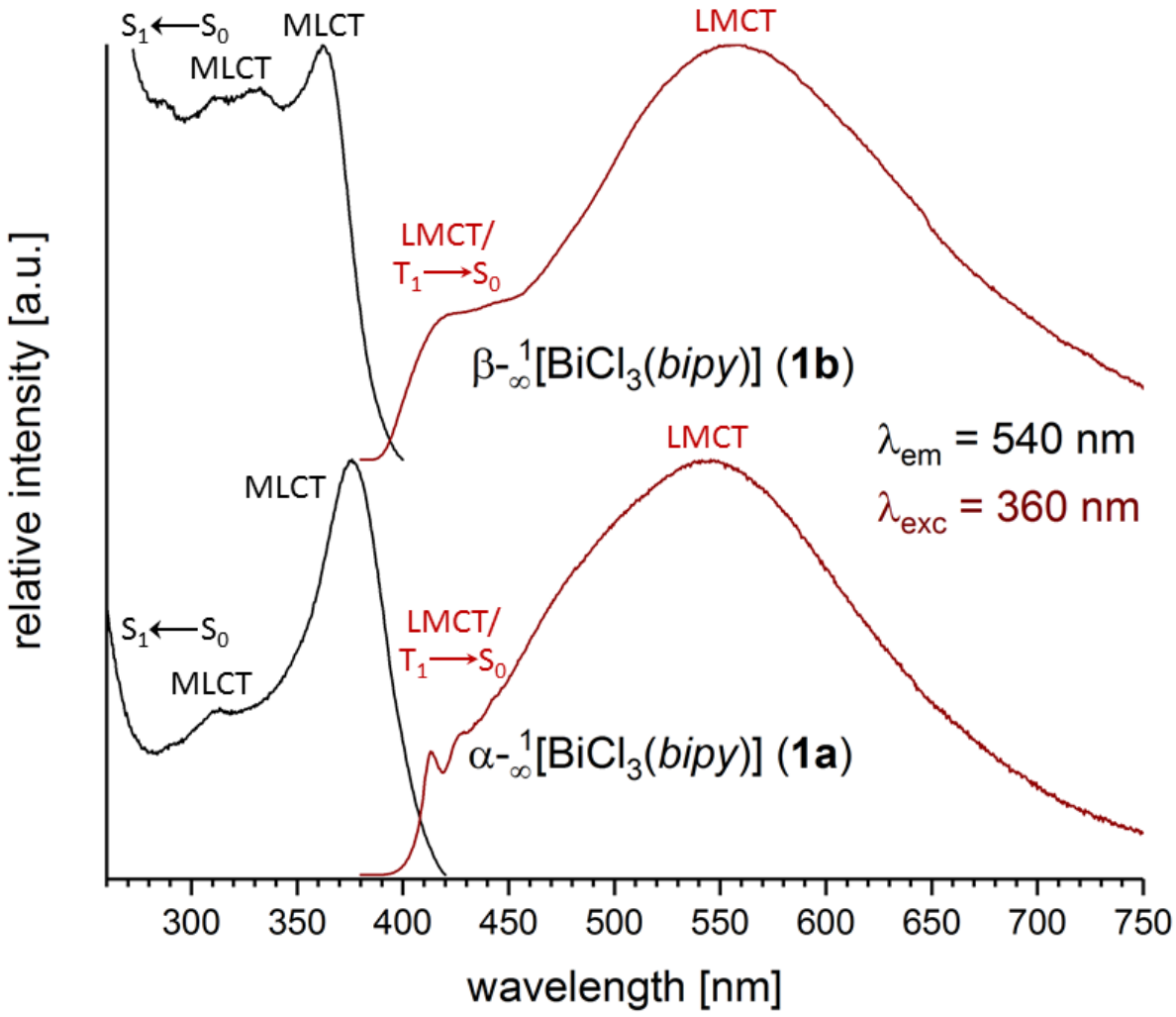

Figure S29. Excitation (black) and emission spectra (red) of α-$^{1}_{\infty}$[Bi_2Cl_6(*bipy*)$_2$] (**1a**) and β-$^{1}_{\infty}$[Bi_2Cl_6(*bipy*)$_2$] (**1b**) recorded at room temperature.

Optical absorption spectra were recorded on a *Varian Cary 5000* UV/Vis/NIR spectrometer in the range of 800-200 nm in diffuse reflectance mode employing a Praying Mantis accessory (*Harrick*).

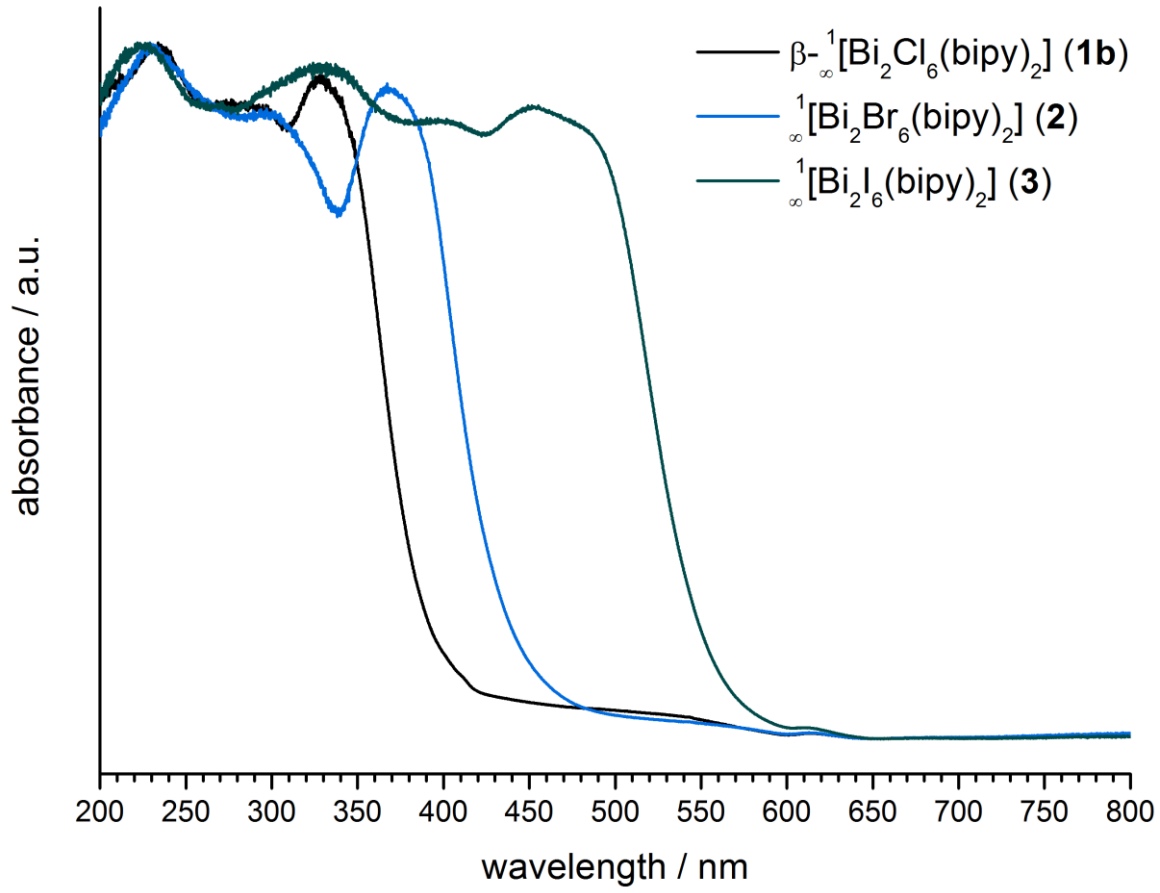

Figure S30. Comparison of the UV-Vis-spectra of **1b, 2** and **3**.

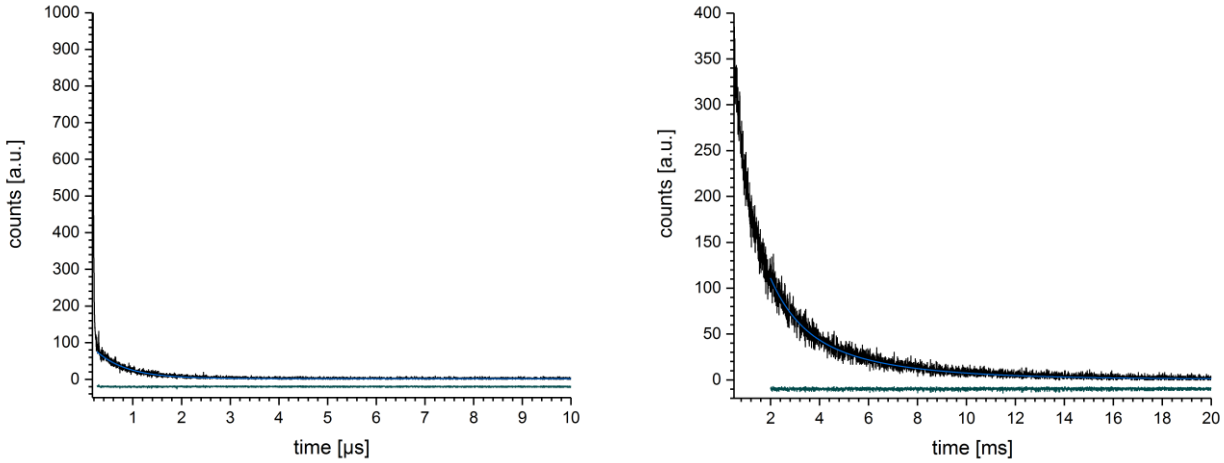

Figure S31. Decay curves (black), exponential fit curves (blue) and difference plot (teal) of emission at 430 nm (left) and 550 nm (right) of α-$^{1}_{\infty}$[Bi_2Cl_6(*bipy*)$_2$] (**1a**) at room temperature.

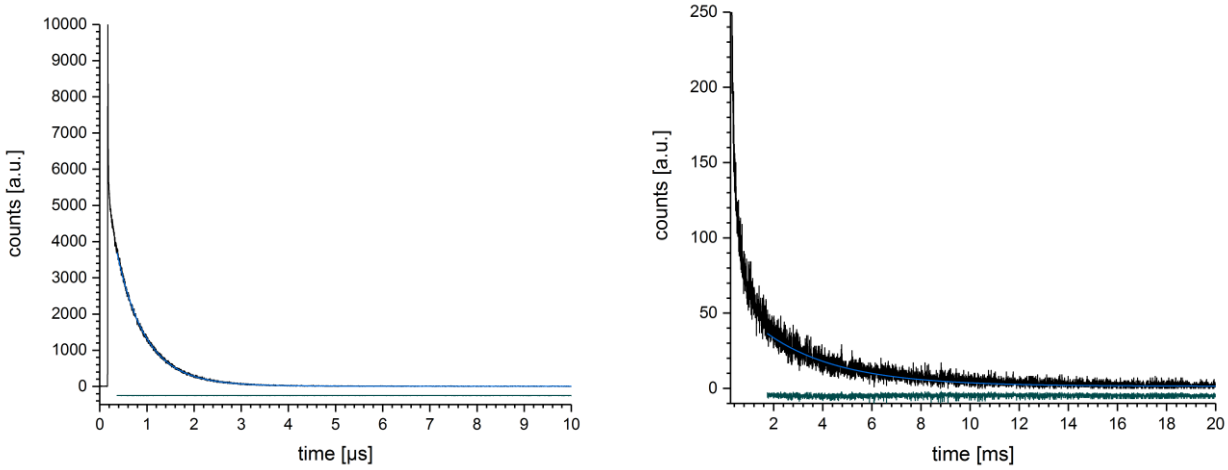

Figure S32. Decay curves (black), exponential fit curves (blue) and difference plot (teal) of emission at 430 nm (left) and 550 nm (right) of β-$^{1}_{\infty}$[Bi_2Cl_6(*bipy*)$_2$] (**1b**) at room temperature.

Table S24: Details of decay time and quantum yield determinations on compounds **1a** and **1b** at room temperature.

Compound	λ_{em} / nm	λ_{exc} / nm	τ	Standard deviation	χ^2	QY / %
α-$^{1}_{\infty}$[Bi_2Cl_6(*bipy*)$_2$] (**1a**)	430	376.6	635.49 ns	6.44 ns	1.076	< 1
	550	365	1184.05 µs (49.4 %) 3750.65 µs (50.6 %)	91.46 µs 146.37 µs	1.081	
β-$^{1}_{\infty}$[Bi_2Cl_6(*bipy*)$_2$] (**1b**)	430	376.6	568.50 ns (84.3 %) 934.28 ns (15.7 %)	114.87 ns 118.59 ns	1.144	< 1
	550	365	3016.12 µs	39.85 µs	1.151	

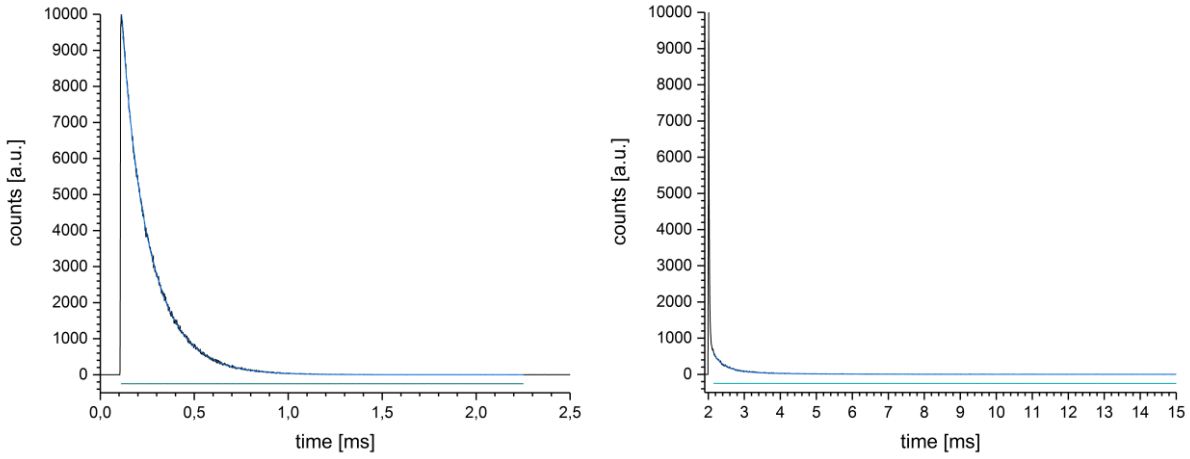

Figure S33. Decay curves (black), exponential fit curves (blue) and difference plot (teal) of emission at 411 nm (left) and 550 nm (right) of α-$^{1}_{\infty}$[Bi_2Cl_6(*bipy*)$_2$] (**1a**) at 77K.

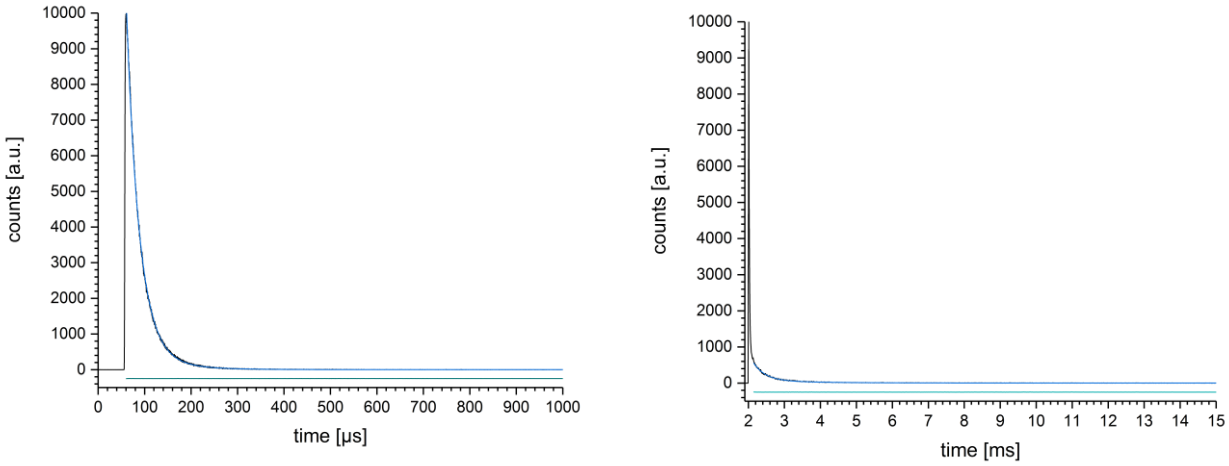

Figure S34. Decay curves (black), exponential fit curves (blue) and difference plot (teal) of emission at 411 nm (left) and 550 nm (right) of β-$^{1}_{\infty}$[Bi_2Cl_6(*bipy*)$_2$] (**1b**) at 77K.

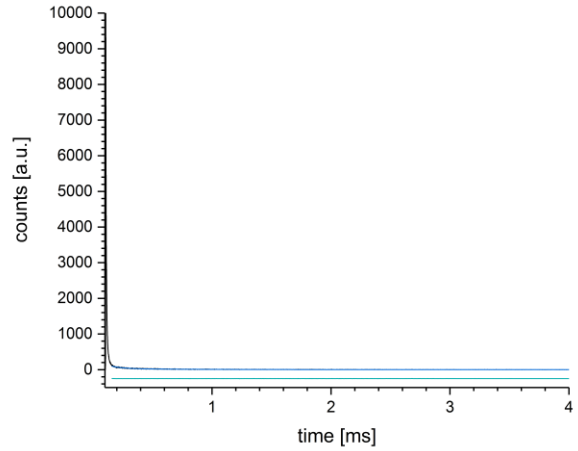

Figure S35. Decay curves (black), exponential fit curves (blue) and difference plot (teal) of emission at 540 nm (right) of $^{1}_{\infty}$[Bi_2Br_6(*bipy*)$_2$] (**2**) at 77K.

Table S25: Details of decay time determinations on compounds **1a**, **1b** and **2** at 77 K.

Compound	λ_{em} / nm	λ_{exc} / nm	τ	Standard deviation	χ^2
α-$^1_\infty$[Bi_2Cl_6(*bipy*)$_2$] (**1a**)	411	365	54.14 µs (12.7 %) 160.26 µs (87.3 %)	2.77 µs 0.33 µs	0.978
	550	365	175.25 µs (88.4 %) 841.63 µs (11.6 %)	3.22 µs 41.76 µs	1.098
β-$^1_\infty$[Bi_2Cl_6(*bipy*)$_2$] (**1b**)	411	365	27.50 µs (94.5 %) 75.88 µs (5.6 %)	0.07 µs 0.74 µs	1.021
	550	365	329.96 µs (86.1 %) 1577.97 µs (13.9 %)	7.10 µs 42.56 µs	0.992
$^1_\infty$[Bi_2Br_6(*bipy*)$_2$] (**2**)	540	400	103.60 µs (6.2 %) 654.88 µs (1.5 %)	4.10 µs 17.89 µs	1.039

Additional Graphics

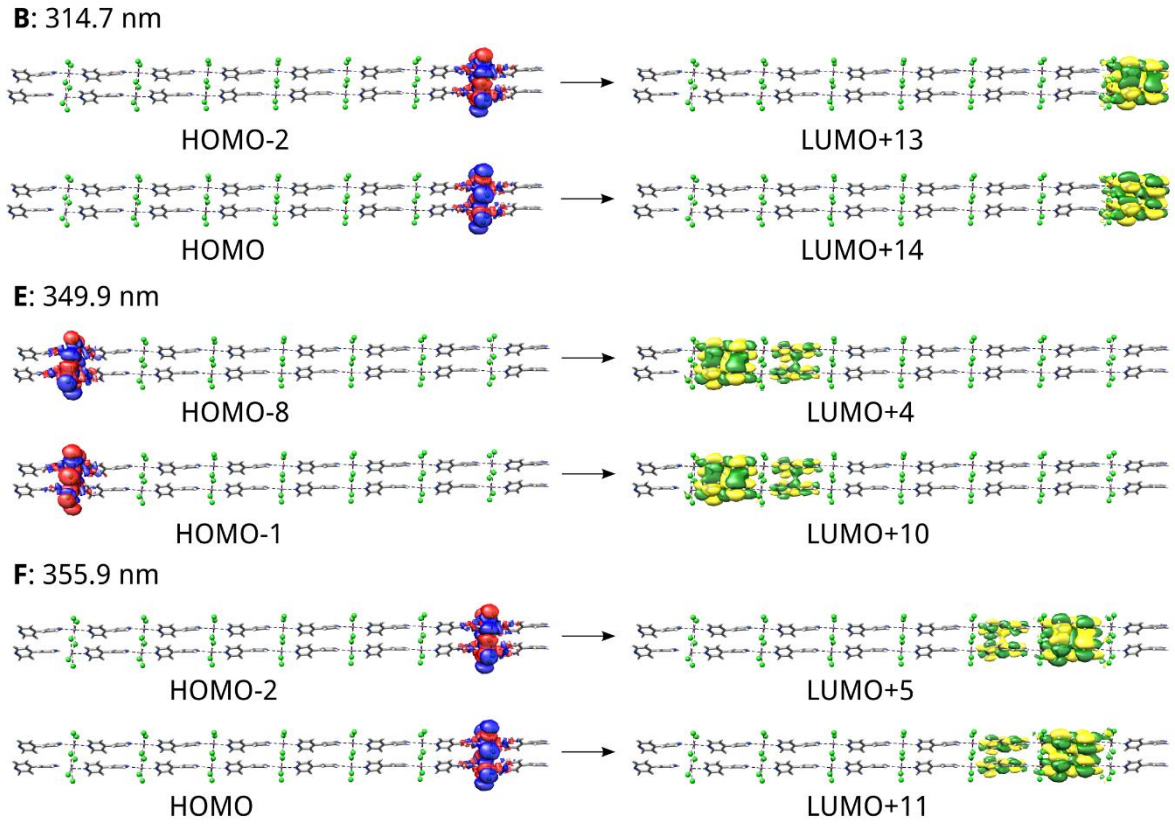

Figure S36. Depictions of the orbitals involved in the vertical transitions of the excitations B, E, and F

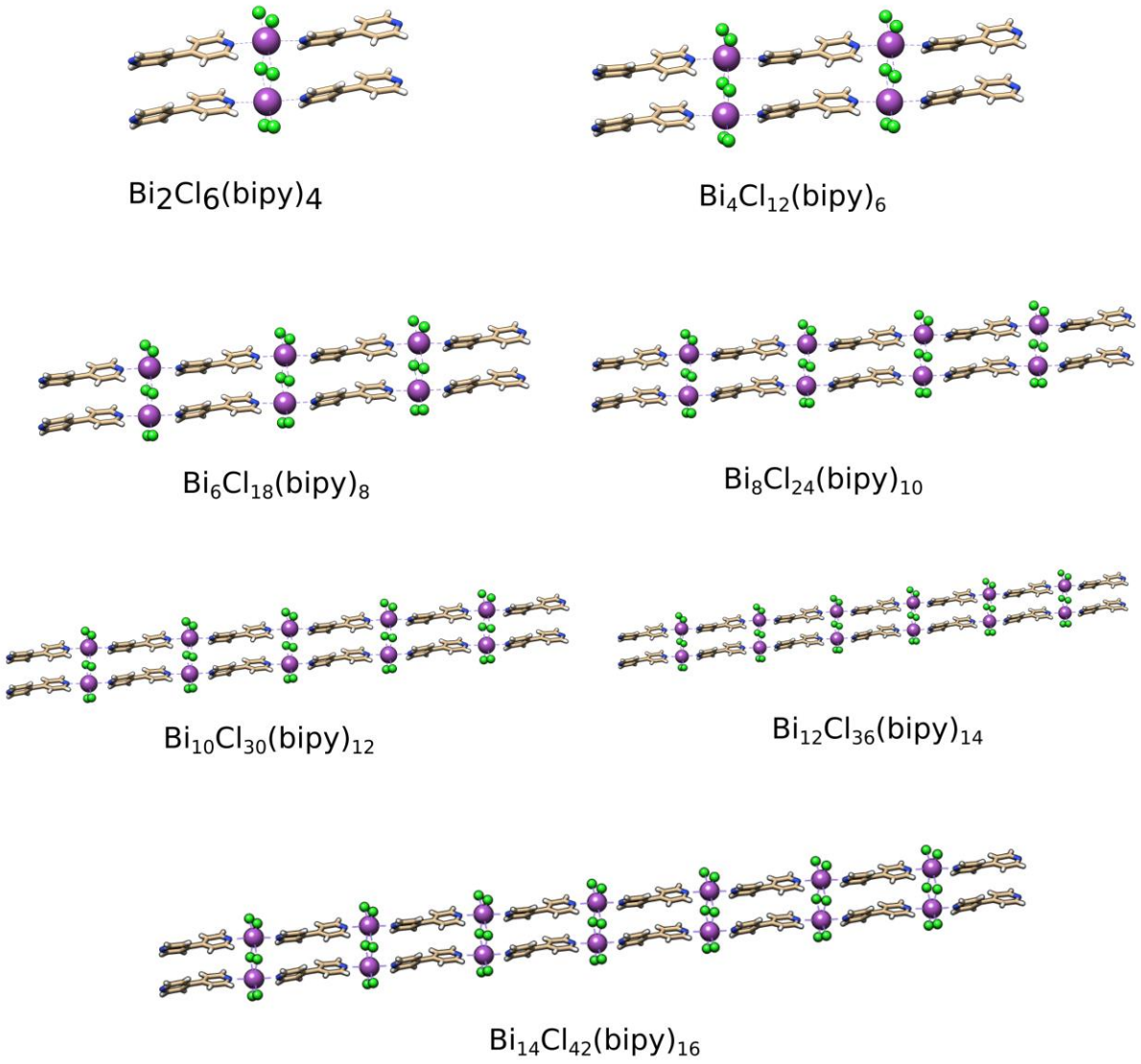

Figure S37. Overview of the seven cut-outs of compound **1a** that were used for theoretical calculations.

References

[1] Heine, J.; Wehner, T.; Bertermann, R.; Steffen, A.; Müller-Buschbaum, K. *Inorg. Chem.* **2014**, *53*, 7197-7203.

[2] Bowmaker, G. A.; Hannaway, F. M. M.; Junk, P. C.; Lee, A. M.; Skelton, B. W.; White, A. H. *Aust. J. Chem.* **1998**, *51*, 325-330.

[3] Lennartson, A.; Hakansson M. CCDC 840295: Experimental Crystal Structure Determination, **2011**, DOI: 10.5517/ccx6d9s.

[4] Höller, C. J.; Mai, M.; Feldmann, C.; Müller-Buschbaum, K. *Dalton Trans.* **2010**, *39*, 461-468.

[5] Matthes, P. R.; Nitsch, J.; Kuzmanoski, A.; Feldmann, C.; Steffen, A.; Marder, T. B.; Müller-Buschbaum, K. *Chem. Eur. J.* **2013**, *19*, 17369-17378.

[6] Matthes, P. R.; Eyley, J.; Klein, J. H.; Kuzmanoski, A.; Lambert, C.; Feldmann, C.; Müller-Buschbaum, K. *Eur. J. Inorg. Chem.* **2015**, *5*, 826-836.

[7] Janiak, C. *J. Chem. Soc., Dalton Trans.* **2000**, *2000*, 3885-3896.